



THE UNIVERSITY *of* EDINBURGH

Edinburgh Research Explorer

Measurement of the production of neighbouring jets in lead–lead collisions at $\sqrt{s_{\mathrm{NN}}} = 2.76\,\mathrm{TeV}$ with the ATLAS detector

Citation for published version:

Clark, PJ, Leonidopoulos, C, Martin, VJ, Mills, C & Collaboration, A 2015, 'Measurement of the production of neighbouring jets in lead–lead collisions at $\sqrt{s_{\mathrm{NN}}} = 2.76\,\mathrm{TeV}$ with the ATLAS detector', *Physics Letters B*, vol. B751, Aad:2015bsa, pp. 376-395. <https://doi.org/10.1016/j.physletb.2015.10.059>

Digital Object Identifier (DOI):

[10.1016/j.physletb.2015.10.059](https://doi.org/10.1016/j.physletb.2015.10.059)

Link:

[Link to publication record in Edinburgh Research Explorer](#)

Document Version:

Publisher's PDF, also known as Version of record

Published In:

Physics Letters B

General rights

Copyright for the publications made accessible via the Edinburgh Research Explorer is retained by the author(s) and / or other copyright owners and it is a condition of accessing these publications that users recognise and abide by the legal requirements associated with these rights.

Take down policy

The University of Edinburgh has made every reasonable effort to ensure that Edinburgh Research Explorer content complies with UK legislation. If you believe that the public display of this file breaches copyright please contact openaccess@ed.ac.uk providing details, and we will remove access to the work immediately and investigate your claim.





Measurement of the production of neighbouring jets in lead–lead collisions at $\sqrt{s_{\text{NN}}} = 2.76$ TeV with the ATLAS detector

ATLAS Collaboration^{*}



ARTICLE INFO

Article history:

Received 29 June 2015

Received in revised form 3 October 2015

Accepted 22 October 2015

Available online 27 October 2015

Editor: D.F. Geesaman

ABSTRACT

This Letter presents measurements of correlated production of nearby jets in Pb+Pb collisions at $\sqrt{s_{\text{NN}}} = 2.76$ TeV using the ATLAS detector at the Large Hadron Collider. The measurement was performed using 0.14 nb⁻¹ of data recorded in 2011. The production of correlated jet pairs was quantified using the rate, $R_{\Delta R}$, of “neighbouring” jets that accompany “test” jets within a given range of angular distance, ΔR , in the pseudorapidity–azimuthal angle plane. The jets were measured in the ATLAS calorimeter and were reconstructed using the anti- k_t algorithm with radius parameters $d = 0.2, 0.3$, and 0.4 . $R_{\Delta R}$ was measured in different Pb+Pb collision centrality bins, characterized by the total transverse energy measured in the forward calorimeters. A centrality dependence of $R_{\Delta R}$ is observed for all three jet radii with $R_{\Delta R}$ found to be lower in central collisions than in peripheral collisions. The ratios formed by the $R_{\Delta R}$ values in different centrality bins and the values in the 40–80% centrality bin are presented.

© 2015 CERN for the benefit of the ATLAS Collaboration. Published by Elsevier B.V. This is an open access article under the CC BY license (<http://creativecommons.org/licenses/by/4.0/>). Funded by SCOAP³.

1. Introduction

Experimental studies of jet production in Pb+Pb collisions at the LHC can directly reveal the properties of the quark–gluon plasma created in the collisions. One predicted consequence of quark–gluon plasma formation is “jet quenching” that refers to the modification of parton showers initiated by hard-scattering processes which take place in the quark–gluon plasma [1]. Measurements of jet pairs at the LHC provided the first direct evidence of jet quenching [2,3]. In those measurements, the enhancement of transverse momentum imbalance of dijets in central Pb+Pb collisions was observed. Measurements at the LHC of inclusive jet suppression [4,5] and the variation of the suppression with jet azimuthal angle with respect to the elliptic flow plane [6] have shown that the transverse energy of jets is significantly degraded and that the energy loss depends on the path length of the parton shower in the plasma. These dijet and single-jet measurements provide complementary information about the jet quenching process. The single jet measurements are sensitive to the average partonic energy-loss while the dijet measurements probe differences in the quenching between the two parton showers traversing the medium. Those differences can arise from the unequal path lengths of the showers in the medium or from fluctuations in the energy loss process itself.

To help disentangle the contributions of these factors to the observed dijet asymmetries, the measurement of the correlations between jets that are at small relative angles was performed. Neighbouring jet pairs include jets originating from the same hard interaction, but also jets from different hard interactions. The latter are not of interest in this analysis, and are subtracted statistically. The remaining neighbouring jet pairs result primarily from hard radiation by the parton that occurs early in the process of the shower formation. Generally, two neighbouring jets originating from the same hard scattering should have more similar path lengths in the medium compared to the two jets in the previous dijet measurement. Therefore measuring neighbouring jets could probe differences in their quenching that do not result primarily from difference in path length. More generally, measurements of the correlated production of jets in the same parton shower may provide more detailed insight into the modification of the parton shower in the quark–gluon plasma beyond the subsequent quenching of the resulting jets.

This Letter presents measurements of the production rate of neighbouring jets in Pb+Pb collisions at $\sqrt{s_{\text{NN}}} = 2.76$ TeV characterized by the quantity $R_{\Delta R}$ introduced in Ref. [7]. The $R_{\Delta R}$ variable quantifies the rate of neighbouring jets that accompany “test” jets within a given range of angular distance, ΔR , in the pseudorapidity–azimuthal angle (η – ϕ) plane,¹ where $\Delta R =$

¹ ATLAS uses a right-handed coordinate system with its origin at the nominal interaction point (IP) in the centre of the detector and the z-axis along the beam pipe.

^{*} E-mail address: atlas.publications@cern.ch.

$\sqrt{(\Delta\eta)^2 + (\Delta\phi)^2}$. Jets were reconstructed with the anti- k_t [8] algorithm using radius parameter values $d = 0.2, 0.3$, and 0.4 . In events with test jets with transverse energy $E_T > 70$ GeV, further jets are searched for within a certain angular distance from the test jet.

The rate of the neighbouring jets that accompany a test jet, $R_{\Delta R}$, is defined as

$$R_{\Delta R}(E_T^{\text{test}}, E_T^{\text{nbr}}) = \frac{\sum_{i=1}^{N_{\text{jet}}^{\text{test}}} N_{\text{jet},i}^{\text{nbr}}(E_T^{\text{test}}, E_T^{\text{nbr}}, \Delta R)}{N_{\text{jet}}^{\text{test}}(E_T^{\text{test}})}, \quad (1)$$

where E_T^{test} and E_T^{nbr} are the transverse energies of the test and neighbouring jet, respectively; $N_{\text{jet}}^{\text{test}}$ is the number of test jets in a given E_T^{test} bin and $N_{\text{jet}}^{\text{nbr}}$ is the number of neighbouring jets. Further, the $R_{\Delta R}$ quantity was used to define per-test-jet normalized spectra of neighbouring jets as

$$\frac{dR_{\Delta R}}{dE_T^{\text{nbr}}} = \frac{1}{N_{\text{jet}}^{\text{test}}} \sum_{i=1}^{N_{\text{jet}}^{\text{test}}} \frac{dN_{\text{jet},i}^{\text{nbr}}}{dE_T^{\text{nbr}}}(E_T^{\text{test}}, E_T^{\text{nbr}}, \Delta R). \quad (2)$$

Previous measurements of the correlated production of neighbouring jets were performed by the DØ experiment in $p\bar{p}$ collisions at the Tevatron [7]. The measurements by DØ were intended to measure the strong coupling constant, α_s , and to test its running over a large range of momentum transfers. The measurements presented in this Letter use similar techniques and follow notations introduced in that measurement.

2. Experimental setup

The measurements presented in this Letter were performed using the ATLAS inner detector, calorimeter, trigger and data acquisition systems [9]. The inner detector [10] measures charged particles within the interval $|\eta| < 2.5$. The inner detector is composed of silicon pixel detectors in the innermost layers, followed by silicon microstrip detectors and a straw-tube tracker, all immersed in a 2 T axial magnetic field provided by a solenoid. The calorimeter system consists of a high-granularity liquid argon (LAr) electromagnetic (EM) calorimeter covering $|\eta| < 3.2$, a steel/scintillator sampling hadronic calorimeter covering $|\eta| < 1.7$, a LAr hadronic calorimeter covering $1.5 < |\eta| < 3.2$. The hadronic calorimeter has three sampling layers longitudinal in shower depth and has a $\Delta\eta \times \Delta\phi$ granularity of 0.1×0.1 for $|\eta| < 2.5$ and 0.2×0.2 for $2.5 < |\eta| < 4.9$.² The EM calorimeters are segmented into three shower-depth compartments with an additional pre-sampler layer. The forward regions are instrumented with copper/LAr and tungsten/LAr forward calorimeters (FCal) covering $3.2 < |\eta| < 4.9$, optimized for electromagnetic and hadronic energy measurements, respectively. Two minimum-bias trigger scintillators (MBTS) counters are located on each side at 3.56 m along the beamline from the centre of the ATLAS detector. The MBTS detect charged particles in the range $2.1 < |\eta| < 3.9$. Each MBTS counter is divided into 16 sections, each of which provides measurements of both the pulse heights and arrival times of energy deposits. The zero-degree calorimeters (ZDCs) are located symmetrically at $z = \pm 140$ m and cover $|\eta| > 8.3$. In Pb+Pb collisions the ZDCs measure primarily

“spectator” neutrons, which originate from one of the incident nuclei and do not interact hadronically with nucleons of the other nucleus.

Minimum-bias Pb+Pb collisions were required either to have the transverse energy in the whole calorimeter exceeding 50 GeV at the Level-1 trigger or to have a track reconstructed in the inner detector in coincidence with ZDC signals on both sides.

Events with high- p_T jets were selected using a combination of a minimum-bias Level-1 trigger and High Level Trigger (HLT) jet triggers. The Level-1 minimum-bias trigger required a total transverse energy measured in the calorimeter to be larger than 10 GeV. The HLT jet trigger used the offline Pb+Pb jet reconstruction described in Section 4, except for the application of the final hadronic energy scale correction. The HLT jet trigger selected events containing a $d = 0.2$ jet with $E_T > 20$ GeV.

3. Event selection and data sets

This analysis used data from Pb+Pb collisions at a nucleon-nucleon centre-of-mass energy of $\sqrt{s_{NN}} = 2.76$ TeV recorded by ATLAS in 2011. It utilizes data samples corresponding to a total integrated luminosity of 0.14 nb^{-1} . The minimum-bias sample was recorded with different prescales depending on the instantaneous luminosity in the LHC fill. The prescale indicates which fraction of events that passed the trigger selection were selected for recording by the DAQ. The minimum-bias trigger recorded an effective luminosity of $7 \mu\text{b}^{-1}$. Events selected by the minimum-bias trigger and the jet triggers were required to have a reconstructed primary vertex with at least three associated tracks each with $p_T > 500$ MeV and a difference between time of pulses from the two sides of the MBTS detector of less than 7 ns. A total of 51 (14.2) million minimum-bias triggered (jet-triggered) events passed the applied event selections and were used in the analysis.

In heavy-ion collisions, “centrality” reflects the overlap volume of the two colliding nuclei, controlled by the impact parameter of the collisions. The centrality of Pb+Pb collisions was characterized by ΣE_T^{FCal} , the total transverse energy measured in the FCal [11]. The centrality intervals were defined according to successive percentiles of the ΣE_T^{FCal} distribution ordered from the most central (highest ΣE_T^{FCal}) to the most peripheral collisions. Production of neighbouring jets was measured in four centrality bins: 0–10%, 10–20%, 20–40%, and 40–80%, with the 40–80% bin serving as the reference. The percentiles were defined after correcting the ΣE_T^{FCal} distribution for a 2% minimum-bias trigger inefficiency that affects the most peripheral events, which are not included in this analysis.

The performance of the ATLAS detector and offline analysis in measuring jets in the environment of Pb+Pb collisions was evaluated using a large sample of Monte Carlo (MC) events obtained by overlaying simulated PYTHIA [12] hard-scattering events onto randomly selected minimum-bias Pb+Pb events, recorded by ATLAS during the same data-taking period as the data used in this analysis. PYTHIA version 6.423 with the AUET2B tune [13] was used. Three million PYTHIA events were produced for each of five intervals of the transverse momentum of outgoing partons in the $2 \rightarrow 2$ hard-scattering process, with boundaries 17, 35, 70, 140, 280, and 560 GeV. The detector response to the PYTHIA events was simulated using GEANT4 [14,15], and the simulated hits were combined with the data from the minimum-bias Pb+Pb events before performing the reconstruction.

4. Jet reconstruction and neighbouring jet selection

Jets were reconstructed within the pseudorapidity interval $|\eta| < 2.8$. The jet reconstruction techniques described in Ref. [4] were used, and are briefly summarized here. The anti- k_t algorithm was

The x-axis points from the IP to the centre of the LHC ring, and the y-axis points upward. Cylindrical coordinates (r, ϕ) are used in the transverse plane, ϕ being the azimuthal angle around the beam pipe. The pseudorapidity is defined in terms of the polar angle θ as $\eta = -\text{Intan}(\theta/2)$.

² An exception is the third sampling layer that has a segmentation of 0.2×0.1 up to $|\eta| = 1.4$.

first run in four-vector recombination mode, on $\Delta\eta \times \Delta\phi = 0.1 \times 0.1$ logical towers. The energies in the towers were obtained by summing energies of calorimeter cells, calibrated at a scale set for electron showers, within the tower boundaries. Then, an iterative procedure was used to estimate a calorimeter layer- and η -dependent underlying event (UE) energy density, while excluding actual jets from that estimate. The UE energy was subtracted from each calorimeter cell within the towers included in the reconstructed jet. The subtraction accounted for a $\cos 2\phi$ modulation in the UE energy density due to collective flow [111] of the medium using a measurement of the amplitude and phase of that modulation in the calorimeter. The jet energies and momenta were calculated via a sum of all cells contained within the jets, treating each cell as a massless four-vector, using E_T values after the UE subtraction. A correction was applied to the reconstructed jet transverse energies to account for jets not excluded or only partially excluded from the UE estimate. The magnitude of the correction was typically a few percent but can be as large as 10% for jets whose energies are fully included in the UE estimate. Then, a final η - and jet E_T -dependent hadronic energy scale calibration factor was applied [4].

Separate from the calorimeter jets, “track jets” were reconstructed by applying the anti- k_t algorithm with $d = 0.4$ to charged particles having $p_T > 4$ GeV. The track jets were used in conjunction with electromagnetic clusters to remove the contribution of “UE jets” generated by fluctuations in the underlying event. The technique is described in detail in Ref. [4].

In the MC simulation, the kinematics of the reference PYTHIA generator-level jets (hereafter called “truth jets”) were reconstructed from PYTHIA final-state particles with the anti- k_t algorithm with radius $d = 0.2, 0.3$, and 0.4 using the same techniques as applied in pp analyses [16]. PYTHIA truth jets were matched to the closest reconstructed jet of the same d value within $\Delta R = 0.2$. The resulting matched jets were used to evaluate the jet energy resolution (JER), the jet energy scale (JES), the jet angular resolution, and the jet reconstruction efficiency.

The $R_{\Delta R}$ measurement was performed with the sample triggered by the jet triggers. The measurement was done differentially in transverse energy of the test and neighbouring jets, and in collision centrality. Five E_T^{test} intervals 70–80, 80–90, 90–110, 110–140, 140–300 GeV and four E_T^{nbr} intervals, 30–45, 45–60, 60–80, 80–130 GeV were used. Furthermore configurations where all the E_T bins of the test jets or of the neighbouring jets have the same upper bound of 300 GeV were also used in this analysis. The number of bins and their boundaries were chosen to minimize the impact of the limited number of events in the data while preserving the ability to infer the trends in the measured distributions. For each jet radius, neighbouring jets are considered if they lie within a specific annulus in ΔR around the test jet: $0.5 < \Delta R < 1.6$, $0.6 < \Delta R < 1.6$, and $0.8 < \Delta R < 1.6$ for $d = 0.2$, $d = 0.3$, and $d = 0.4$ jets, respectively. The inner edge of each annulus was chosen to avoid possible overlap of test and neighbouring jets, and the outer edge value ($\lesssim \pi/2$) rejects neighbouring jets in the hemisphere opposite to the test jet and maximizes the number of events. Choosing a maximum ΔR of 1.6 restricts the pseudorapidity range of test jets to $|\eta| < 1.2$, yielding approximately 87×10^3 $d = 0.4$ test jets with $p_T > 80$ GeV analysed in 0–10% central events and 37×10^3 test jets in 40–80% peripheral events.

To quantify the centrality dependence of the neighbouring jet yields, the ratio $\rho_{R_{\Delta R}} = R_{\Delta R}|_{\text{cent}}/R_{\Delta R}|_{40-80}$ is calculated as the ratio of $R_{\Delta R}$ measured in each centrality bin to $R_{\Delta R}$ measured in the reference (40–80%) bin.

5. Corrections to neighbouring jet rates

The raw rates of neighbouring jets include a contribution from neighbouring jets that originate from different hard partonic interactions in the same Pb+Pb collision. This combinatorial background is present both in the MC simulation and in the data and must be subtracted. It is largest in the low E_T^{nbr} bins and it increases with increasing centrality of the collision, since the probability for the presence of two independent hard scatterings in one Pb+Pb collision is expected to increase with the number of binary collisions. The combinatorial background is estimated using the differential yield of inclusive jets ($d^3N_{\text{jet}}/d\eta d\phi dE_T$) evaluated in minimum-bias Pb+Pb events. To each event considered a weight is assigned such that the event sample obtained from the minimum-bias trigger has the same centrality distribution as the sample collected by the jet trigger. This estimated background needs to be corrected for a geometrical bias present in the case where the combinatorial jet overlaps with a real neighbouring jet or when two combinatorial jets overlap. These biases were removed by applying a multiplicative correction factor to background distributions prior to the subtraction. This multiplicative factor was derived from the reconstruction efficiency of two neighbouring jets evaluated as a function of their angular separation in the annulus. In that evaluation, one jet was required to originate from PYTHIA’s hard scattering and the other jet was required to originate from the minimum-bias data in the overlay. The impact of this correction on the final subtracted distribution is smaller than 0.5%.

The combinatoric jet kinematics may also be affected by the presence of a test jet. To control this influence, a study comparing the combinatoric jets from the overlay MC events with the same jets in the original minimum-bias data was performed. This study resulted in an additional correction, independent of centrality and jet E_T , that decreases the combinatorial background by 1.5%. The $\pm 1.2\%$ uncertainty on the correction originates from the limited number of events and was included in the systematic uncertainties.

In order to account for the effect of the azimuthal dependence of jet yields [6], the combinatorial background was reweighted to take into account the measured azimuthal distributions of test jets as well as combinatorial jets. The change of the raw subtracted distribution in central collisions and low E_T^{nbr} bins after the reweighting is at the level of 1% and decreases with increasing centrality of the collision and E_T^{nbr} .

The background is subtracted from raw $R_{\Delta R}$ distributions both in the data and in the MC simulation, allowing an evaluation of the effectiveness of the subtraction using the MC simulation. The signal-to-background ratio strongly depends on the centrality of the collision and E_T^{nbr} . In 0–10% central collisions, the signal-to-background ratio can be as low as 0.15 for the most extreme case of $30 < E_T^{\text{nbr}} < 45$ GeV, and increases to approximately 0.8 for $60 < E_T^{\text{nbr}} < 80$ GeV.

The raw subtracted $R_{\Delta R}$ distributions are affected by the jet energy resolution. The combination of the jet energy resolution and the steeply falling E_T spectrum produces a net migration of jets from lower E_T to higher E_T values such that a jet reconstructed with a given E_T^{rec} corresponds, on average, to a lower truth jet E_T , $\langle E_T^{\text{truth}} \rangle$. The relationship between $\langle E_T^{\text{truth}} \rangle$ and E_T^{rec} was evaluated in simulated events for the different centrality bins and three jet radii used in the analysis. The extracted relationships were used to correct for the average shift in the test jet energy. No correction due to the jet reconstruction efficiency for the test jets is needed, since the analysis operates in the transverse energy region where the jet reconstruction is fully efficient. No correction due to jet trigger efficiency is needed either since the plateau of the jet trigger efficiency is reached for all test jets, except for $d = 0.4$ jets

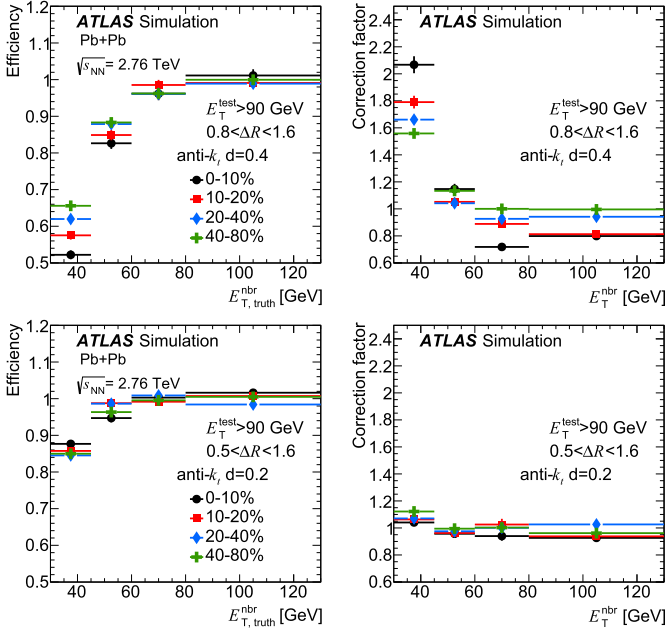


Fig. 1. Reconstruction efficiency (left) of neighbouring jets as a function of the transverse energy of the neighbouring jet at Monte Carlo generator level $E_{T, \text{truth}}^{\text{nbr}}$ and bin-by-bin correction factors for the distributions of the neighbouring jet rate $R_{\Delta R}$ (right) as a function of the reconstructed transverse energy of the neighbouring jet E_T^{nbr} . Plots for two different jet radii, $d = 0.4$ (upper plots) and $d = 0.2$ (lower plots) are shown and the transverse energy of the test jet E_T^{test} is required to exceed 90 GeV. The four different centrality bins are denoted by different markers in each plot. The vertical error bars represent statistical uncertainties.

with $E_T^{\text{test}} < 90$ GeV in the 0–10% and 10–20% centrality bins. In the region $70 < E_T < 90$ GeV, the jet trigger efficiency is above 85%. A systematic uncertainty is applied to describe the effect of the lower jet reconstruction efficiency.

The impact of the jet energy resolution, reconstruction efficiency, and angular resolution on neighbouring jet yields is corrected for by applying bin-by-bin unfolding to the raw subtracted $R_{\Delta R}$ distributions. For each measured $R_{\Delta R}$ distribution, two corresponding MC distributions are evaluated, one using truth jets and the other using jets after the detector simulation. The ratio of these two MC distributions provides a correction factor which is then applied to the data.

The bin-by-bin correction factors are derived from the MC simulation where the reconstructed jets were matched to the truth jets. To account for the impact of the jet angular resolution, the truth jet is required to lie within a given annulus while the reconstructed jet is allowed to fall outside of the annulus.

Examples of jet reconstruction efficiencies for neighbouring jets and the bin-by-bin correction factors accounting for the efficiency and resolution effects are shown in Fig. 1 for different centrality selections and for two choices of jet radii: $d = 0.4$ and $d = 0.2$. Generally, the jet energy resolution in central (0–10%) collisions for $d = 0.4$ jets has comparable contributions from UE fluctuations and the “intrinsic” resolution of the calorimetric jet measurement. The fluctuations in the UE are approximately two times smaller for $d = 0.2$ jets than they are for $d = 0.4$ jets. Thus, the distributions measured using $d = 0.2$ jets are far less sensitive to the effects of the jet energy resolution, and consequently the resulting bin-by-bin correction factors for those distributions exhibit only a modest centrality dependence. The difference in the jet reconstruction efficiency between the two choices of jet radii is also significant – the efficiency for $d = 0.2$ jets plateaus around 30 GeV, where it is still rising rapidly for $d = 0.4$ jets.

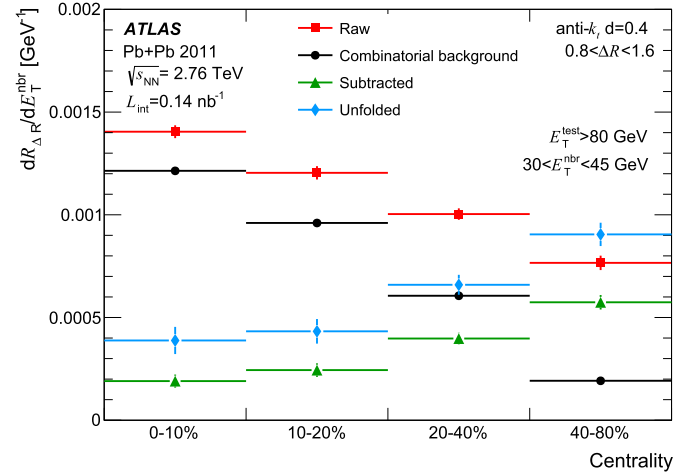


Fig. 2. Summary of how the corrections impact the $dR_{\Delta R}/dE_T^{\text{nbr}}$ distribution measured in the data in different centrality bins. The $dR_{\Delta R}/dE_T^{\text{nbr}}$ is shown for $d = 0.4$ jets for $E_T^{\text{test}} > 80$ GeV and in the interval $30 < E_T^{\text{nbr}} < 45$ GeV. Squares show the raw $dR_{\Delta R}/dE_T^{\text{nbr}}$ prior to the UE subtraction, circles show the combinatorial background, triangles show the subtracted $dR_{\Delta R}/dE_T^{\text{nbr}}$ prior to unfolding by applying the bin-by-bin correction factors, and diamonds show the unfolded $dR_{\Delta R}/dE_T^{\text{nbr}}$. Vertical error bars on the combinatorial background, raw, and subtracted distributions represent statistical uncertainties. Vertical error bars on the unfolded distribution represent the combined statistical uncertainty from the unfolding and from subtracted distributions.

The jet angular resolution is determined in MC simulation as the standard deviation of the difference in angles between truth and reconstructed jets. In both η and ϕ it reaches 0.008 in 0–10% collisions and 0.005 in the 40–80% centrality bin for $d = 0.4$ jets with $E_T = 30$ GeV. The angular resolution improves with increasing jet E_T and reaches 0.004 (resolution in η) and 0.002 (resolution in ϕ) at $E_T = 200$ GeV, independently of centrality.

The impact of these corrections on $R_{\Delta R}$ distributions measured in the data in different centrality bins is shown in Fig. 2. The figure shows the raw $R_{\Delta R}$ distribution, and the combinatorial background, subtracted, and final unfolded $R_{\Delta R}$ distributions for $d = 0.4$ jets with $E_T^{\text{test}} > 80$ GeV and in the lowest E_T^{nbr} interval, $30 < E_T^{\text{nbr}} < 45$ GeV. The raw $R_{\Delta R}$ distribution increases from peripheral to central collisions. The increase of the combinatorial background is steeper than the increase of the raw distribution. Therefore, a decrease of subtracted $R_{\Delta R}$ with increasing collision centrality is observed. The trend in the centrality dependence of the $R_{\Delta R}$ distribution remains unchanged when the bin-by-bin correction is applied.

6. Systematic uncertainties

Systematic uncertainties in the measurement of $R_{\Delta R}$ distributions and their ratios, $\rho_{R_{\Delta R}}$, arise from the uncertainty on the jet energy scale, jet energy resolution, angular resolution, bin-by-bin unfolding, centrality, combinatorial background and jet trigger efficiency. The impact of uncertainties on the jet energy scale, jet energy resolution and jet angular resolution was assessed by constructing new bin-by-bin correction factors with a systematically varied relationship between the reconstructed and truth jet kinematics. The resulting uncertainties on $R_{\Delta R}$ and $\rho_{R_{\Delta R}}$ were evaluated from their changed values obtained with modified jet energy scale, jet energy resolution and jet angular resolution dependencies.

The systematic uncertainty due to the jet energy scale is composed of two parts: an absolute, centrality-independent compo-

nent, and a centrality-dependent component. The uncertainty on $R_{\Delta R}$ from the jet energy scale uncertainty is evaluated by shifting all reconstructed jet transverse energies by ± 1 standard deviation of the jet energy scale uncertainty. The absolute component is determined from the *in situ* studies of the calorimeter response; systematic variations of the jet response in the MC simulation [16]; and from studies of the relative energy scale difference between the jet reconstruction procedure in heavy-ion collisions, and the procedure used for inclusive jet measurements in 2.76 TeV and 7 TeV *pp* collisions [17]. The magnitude of the uncertainty on the $R_{\Delta R}$ from the absolute jet energy scale uncertainty varies from 2% to 15% as a function of E_T and radius of the jet. The centrality-dependent component of jet energy scale uncertainty [5] was estimated using the PYQUEN MC generator [18]. The PYQUEN MC generator was tuned with the Pro-Q20 tune [19] to provide a sample of jets with modified fragmentation functions consistent with measurements in quenched jets performed by ATLAS [20] and CMS [21] as documented in Ref. [17].

The centrality-dependent jet energy scale uncertainty reaches 1% for 0–10% central collisions and less than 0.25% for 40–80% peripheral collisions. The uncertainty on $R_{\Delta R}$ originating from the centrality-dependent component of the jet energy scale uncertainty increases from less than 1% in peripheral collisions to 3% in central collisions.

The effect of the jet energy resolution uncertainty was evaluated by applying modified bin-by-bin correction factors where the reconstructed jet E_T was smeared. The uncertainty on the jet energy resolution is dominated by the uncertainty in the detector response. Thus, the procedure used for jet measurements in the 7 TeV *pp* collisions [16] is used. The smearing factor is evaluated using an *in situ* technique involving studies of dijet energy balance. The systematic uncertainty on $R_{\Delta R}$ due to the jet energy resolution varies from 1% to 4% depending on the jet E_T . The centrality-independent jet energy scale uncertainty and the uncertainty from jet energy resolution tend to cancel in the $\rho_{R_{\Delta R}}$ ratios since both the numerator and denominator in the ratios are affected to a similar degree by the variations accounting for the uncertainties.

The systematic uncertainty on combinatorial contributions originates from the previously noted uncertainty on the correction factor taking into account the difference between jets in minimum-bias events and combinatorial jets in the overlay. The resulting uncertainty reaches $\sim 8\%$ in 0–10% central collisions at low E_T^{nbr} and rapidly decreases with decreasing centrality or increasing E_T^{nbr} .

The systematic uncertainty associated with the bin-by-bin unfolding is connected with possible differences in the spectral shape between the data and the MC simulation. To achieve better correspondence with the data, the simulated jet spectrum was reweighted to match the spectral shape in the data before deriving the bin-by-bin correction factors as described above. Conservatively, the entire change in $R_{\Delta R}$ and $\rho_{R_{\Delta R}}$ induced by the use of reweighted bin-by-bin correction factors is taken as a systematic uncertainty. Typically, this results in 1–2% uncertainty on $R_{\Delta R}$. A maximum uncertainty of 5% is reached in 0–10% central collisions for $R_{\Delta R}$ evaluated for neighbouring jets with $E_T^{\text{nbr}} > 30$ GeV.

The uncertainty on the centrality estimation originates from the uncertainty on the estimated inefficiency of the minimum-bias trigger. The analysis was repeated with modified centrality bins assuming 100% minimum-bias trigger efficiency. The resulting uncertainty is typically smaller than 5% with a mild E_T dependence and a negligible centrality dependence.

The uncertainty associated with the jet angular resolution is estimated using modified bin-by-bin correction factors where the

Table 1

Maximum systematic uncertainties on $R_{\Delta R}$ ($\delta R_{\Delta R}$) and on the ratio of $R_{\Delta R}$ in central collisions and in peripheral (40–80%) collisions $\rho_{R_{\Delta R}}$ ($\delta \rho_{R_{\Delta R}}$) for $d = 0.4$ jets in the 0–10% and 40–80% centrality bins. The systematic uncertainty on the trigger is applicable only for $E_T^{\text{test}} < 90$ GeV.

	$\delta R_{\Delta R}$		$\delta \rho_{R_{\Delta R}}$
	0–10%	40–80%	0–10%
JES	15%	11%	7%
JER	4%	2%	2%
Angular resolution	2%	0.5%	2%
Unfolding	5%	2%	5%
Centrality	6%	6%	6%
Combinatoric	8%	<0.5%	8%
Trigger	5%	–	5%

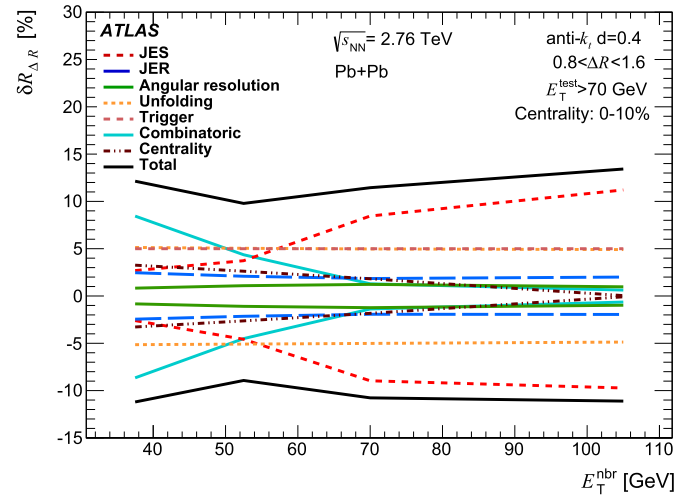


Fig. 3. Summary of the relative systematic uncertainties, in %, on the $R_{\Delta R}$ distributions ($\delta R_{\Delta R}$). The systematic uncertainties due to the jet energy scale (JES), the jet energy resolution (JER), the jet angular resolution, unfolding, jet trigger efficiency, combinatorial contributions and centrality are shown for $d = 0.4$ jets with $E_T^{\text{test}} > 70$ GeV in 0–10% central collisions.

reconstructed jet η and ϕ is smeared to reflect a up to $\sim 15\%$ centrality and E_T dependent uncertainty on the angular resolution. The uncertainty on the jet angular resolution was estimated by comparing the angular distance between track jets and the closest calorimetric jet in the data and in the MC simulation. The magnitude of uncertainty on $R_{\Delta R}$ from the jet angular resolution is smaller than 2%.

The systematic uncertainty on the jet trigger efficiency covers a possible bias caused by selecting test jets in the region where the jet trigger is not fully efficient. This is the case for the $d = 0.4$ jets with $E_T^{\text{test}} < 90$ GeV reconstructed in the 0–10% and 10–20% centrality bins. For that E_T region, the systematic uncertainty was determined as the difference between the trigger efficiencies for inclusive jets and jets that were required to have a neighbouring jet. This trigger efficiency difference is less than 5% and is independent of the E_T^{nbr} .

To avoid statistical fluctuations in the values of systematic uncertainties, the weak E_T^{nbr} dependence of the uncertainties is smoothed by a second-order polynomial. Systematic uncertainties on $R_{\Delta R}$ for $d = 0.4$ jets are summarized in Table 1 for the 0–10% and 40–80% centrality bins. The table shows the maximum values of uncertainties for $R_{\Delta R}$ and for $\rho_{R_{\Delta R}}$. The total systematic uncertainties for jets with the other two jet radii are smaller than those shown in the table. For the 0–10% centrality bin these systematic uncertainties are also plotted in Fig. 3 as a function of E_T^{nbr} .

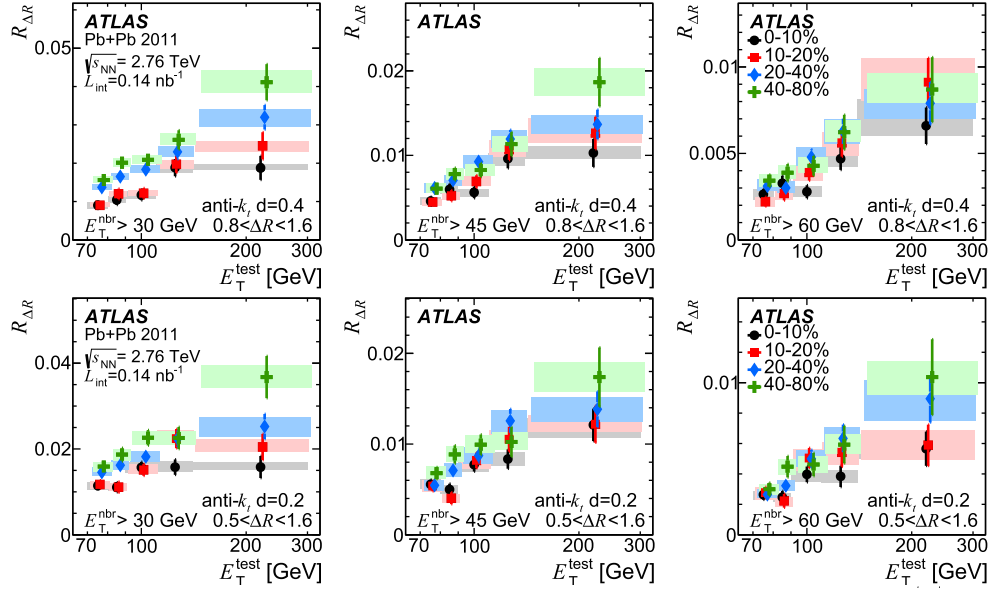


Fig. 4. $R_{\Delta R}$ distributions for $d = 0.4$ jets (upper) and $d = 0.2$ jets (lower) evaluated as a function of E_T^{test} . The three different columns show $R_{\Delta R}$ distributions evaluated for three different lower bounds on the neighbouring-jet transverse energy, $E_T^{\text{nbr}} > 30, 45$, and 60 GeV. The four different centrality bins are denoted by different markers in each plot. The shaded bands indicate systematic uncertainties, vertical error bars represent statistical uncertainties, the horizontal size of the systematic uncertainties indicates the bin width. The data points and horizontal uncertainties for the 10–20%, 20–40%, and 40–80% centrality bins are shifted along the horizontal axis with respect to the 0–10% centrality bin for clarity.

7. Results

The $R_{\Delta R}$ measurement is performed differentially in collision centrality, transverse energy of the test jet, E_T^{test} , and transverse energy of the neighbouring jet, E_T^{nbr} , as described Section 4. The measured distributions are divided into four centrality bins, 0–10%, 10–20%, 20–40%, and 40–80%. Fig. 4 shows the fully corrected $R_{\Delta R}$ distributions for $d = 0.4$ and $d = 0.2$ jets evaluated as a function of E_T^{test} . The distributions are shown for four centrality bins and three different lower bounds on the neighbouring-jet transverse energy, $E_T^{\text{nbr}} > 30, 45$, and 60 GeV. The shaded error bands on the plots indicate the systematic uncertainties discussed in Section 6. The $R_{\Delta R}$ distribution exhibits an increase with increasing E_T^{test} , which is consistent in shape with the previous measurement of the same quantity by DØ in pp collisions. Sizeable differences between the four different centrality bins are observed for all three jet radii. The yield of neighbouring jets is suppressed as the centrality of the collision increases.

To further investigate the centrality dependence of neighbouring jet yields, the per-test-jet normalized E_T spectra of neighbouring jets defined in Eq. (2) were evaluated. The resulting differential E_T spectra are shown in Fig. 5 for $d = 0.4$ and $d = 0.2$ jets and three different lower bounds on the test-jet transverse energy, $E_T^{\text{test}} > 80, 90$, and 110 GeV. The same trend of suppression in central collisions can be seen as that for $R_{\Delta R}$ evaluated as a function of test-jet transverse energy shown in Fig. 4. This is a consequence of the steeply falling shape of the E_T spectra. To better quantify the differences in the E_T spectra of neighbouring jets, the E_T spectra were fitted to a power-law function, $\propto 1/E_T^n$, and the power index was extracted for all three choices of jet radius and four centrality bins. The results are given in Table 2. The E_T spectra measured in central and peripheral collisions differ in the power-law index by approximately two standard deviations for both the $d = 0.4$ and $d = 0.3$ jets, suggesting that the E_T spectra may be less steep in central collisions than in peripheral collisions.

To quantify the centrality dependence of the suppression of neighbouring jets, the ratios $\rho_{R_{\Delta R}}$ were calculated by dividing $R_{\Delta R}$ measured in each centrality bin, except the peripheral bin, by $R_{\Delta R}$

Table 2

Power-law index n extracted from fits of $dR_{\Delta R}/dE_T^{\text{nbr}}$ distributions to a power-law function $\propto 1/E_T^n$ for $E_T^{\text{test}} > 90$ GeV, for four bins in centrality and three jet radii. The resulting fit error takes into account combined statistical and systematic uncertainties.

	0–10%
$d = 0.4$	$2.73 \pm 0.23(\text{stat.}) \pm 0.12(\text{syst.})$
$d = 0.3$	$2.83 \pm 0.16(\text{stat.}) \pm 0.14(\text{syst.})$
$d = 0.2$	$2.81 \pm 0.15(\text{stat.}) \pm 0.15(\text{syst.})$
	10–20%
$d = 0.4$	$2.85 \pm 0.17(\text{stat.}) \pm 0.13(\text{syst.})$
$d = 0.3$	$2.51 \pm 0.15(\text{stat.}) \pm 0.11(\text{syst.})$
$d = 0.2$	$2.56 \pm 0.16(\text{stat.}) \pm 0.12(\text{syst.})$
	20–40%
$d = 0.4$	$2.90 \pm 0.12(\text{stat.}) \pm 0.10(\text{syst.})$
$d = 0.3$	$2.91 \pm 0.11(\text{stat.}) \pm 0.09(\text{syst.})$
$d = 0.2$	$2.62 \pm 0.13(\text{stat.}) \pm 0.10(\text{syst.})$
	40–80%
$d = 0.4$	$3.26 \pm 0.15(\text{stat.}) \pm 0.13(\text{syst.})$
$d = 0.3$	$3.24 \pm 0.15(\text{stat.}) \pm 0.11(\text{syst.})$
$d = 0.2$	$2.99 \pm 0.17(\text{stat.}) \pm 0.11(\text{syst.})$

measured in the peripheral (40–80%) bin. Fig. 6 shows $\rho_{R_{\Delta R}}$ evaluated as a function of E_T^{test} and E_T^{nbr} . Some systematic uncertainties cancel in the central-to-peripheral ratio as described in Section 6, resulting in $\rho_{R_{\Delta R}}$ distributions that are dominated by statistical uncertainties. Ratios are evaluated for $d = 0.4$ jets, which suffer the least from the statistical uncertainties, that are still large. Nevertheless, several characteristic features can be observed: the $\rho_{R_{\Delta R}}$ distributions do not exhibit any strong dependence on E_T^{test} ; the suppression factor $\rho_{R_{\Delta R}}$ of the most central collisions is at the level of 0.5–0.7 for all three lower bounds on E_T^{nbr} ; the suppression seems to become less pronounced with decreasing centrality. This is qualitatively consistent with the observation of the centrality-dependent suppression of inclusive jet yields [4]. In that measurement, the suppression of the inclusive jet yields was evaluated in terms of the ratio R_{CP} of the inclusive jet yield in central collisions

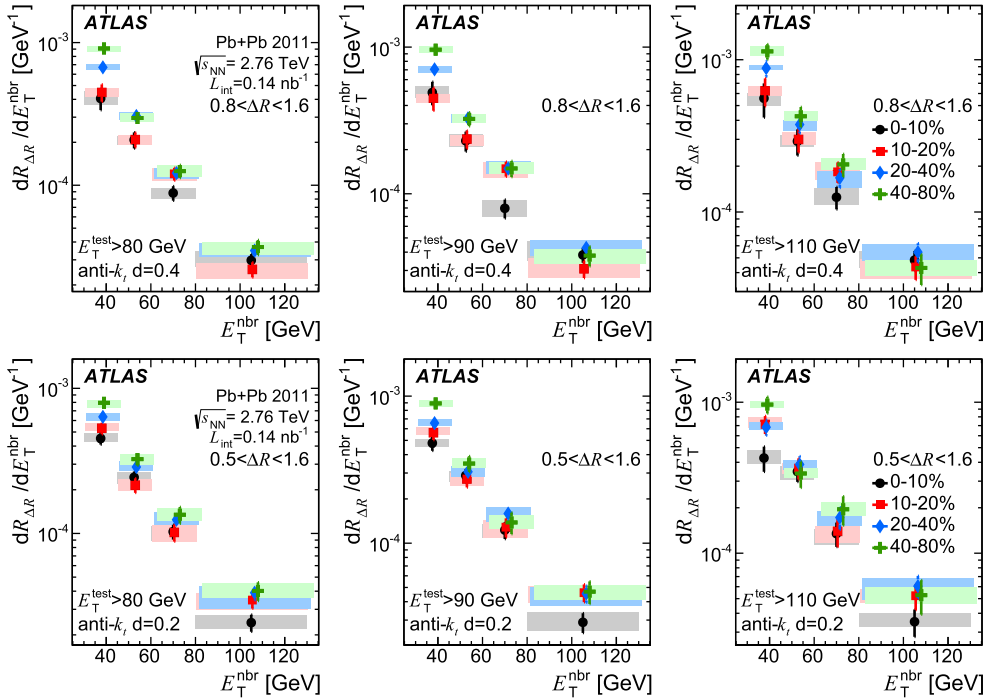


Fig. 5. The $dR_{\Delta R}/dE_T^{nbr}$ distributions for $d = 0.4$ jets (upper) and $d = 0.2$ jets (lower) evaluated as a function of E_T^{nbr} . The three different columns show the $dR_{\Delta R}/dE_T^{nbr}$ distributions evaluated for three different lower bounds on the test-jet transverse energy, $E_T^{test} > 80, 90$, and 110 GeV. The four different centrality bins are denoted by different markers in each plot. The shaded bands indicate systematic uncertainties, vertical error bars represent statistical uncertainties, the horizontal size of the systematic uncertainties indicates the bin width. The data points and horizontal uncertainties for 10–20%, 20–40%, and 40–80% centrality bins are shifted along the horizontal axis with respect to 0–10% centrality bin for clarity.

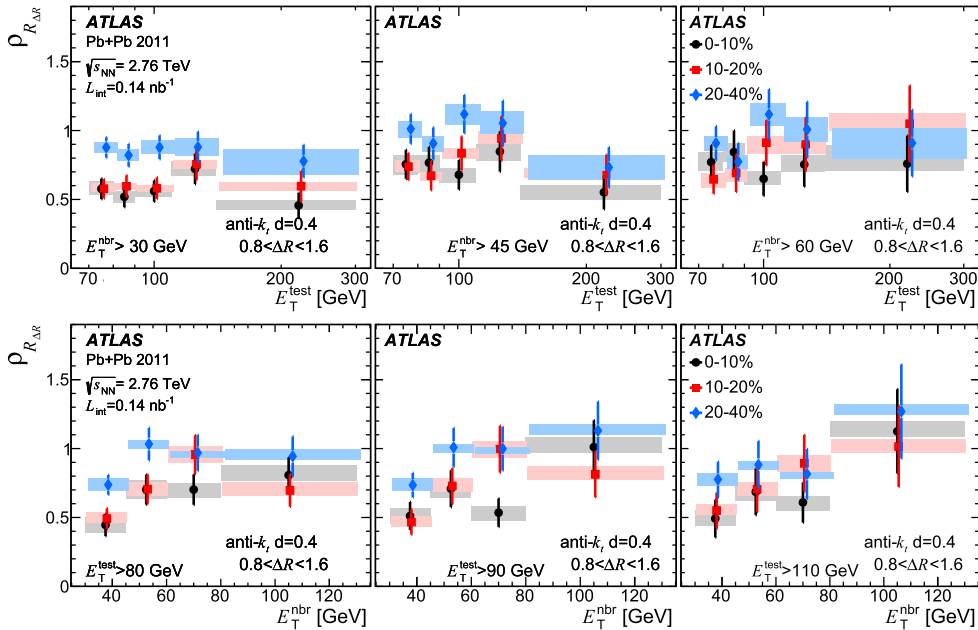


Fig. 6. The ratio of $R_{\Delta R}$ for three bins of collision centrality to those in 40–80 collisions, $\rho_{R_{\Delta R}} = R_{\Delta R|cent}/R_{\Delta R|40-80}$ for $d = 0.4$ jets. The $\rho_{R_{\Delta R}}$ is evaluated as a function of E_T^{test} for three different choices of lower bound on E_T^{nbr} (upper) and as a function of E_T^{nbr} for three different choices of lower bound on E_T^{test} (lower). The shaded bands indicate systematic uncertainties, vertical error bars represent statistical uncertainties, the horizontal size of the systematic uncertainties indicates the bin width. The data points and horizontal uncertainties for 10–20%, 20–40%, and 40–80% centrality bins are shifted along the horizontal axis with respect to 0–10% centrality bin for clarity.

sions to the yield in 60–80% peripheral collisions spanning the jet p_T range of 40–200 GeV. Values of $R_{CP} \sim 0.5$ were measured in the 0–10% most central collisions and exhibited only a weak jet- p_T dependence.

Contrary to a modest dependence of $\rho_{R_{\Delta R}}$ on the test-jet E_T , the $\rho_{R_{\Delta R}}$ evaluated as a function of E_T^{nbr} suggests a decrease of

suppression with increasing E_T^{nbr} . Such a decrease in suppression with increasing E_T^{nbr} may in fact be expected. The jet quenching is generally expected to depend on the initial parton energy, but if the splitting happens such that the two partons have similar energy, their quenching would likely be comparable due to similar in-medium path-length travelled by the two partons forming

neighbouring jets. Thus, in the configuration of $E_T^{\text{nbr}} \approx E_T^{\text{test}}$ the per-test-jet normalization effectively removes the impact of the suppression.

8. Conclusions

This Letter presents results of a measurement of the production of neighbouring jets using pairs of jets produced at opening angles less than $\pi/2$ in η – ϕ plane. After subtraction of combinatorial backgrounds from different hard-scattering processes, such jet pairs result from the production of multiple jets in the same hard-scattering process. As such, it is complementary to previous studies of single-jet suppression and dijet asymmetry. By probing the relative quenching of a pair of correlated jets in different collision centralities, this measurement opens up the possibility to study the role of fluctuations in the jet quenching process. This measurement represents a first, exploratory study of how the quark-gluon plasma influences the production and/or later evolution of the neighbouring jets from the same parton shower in heavy-ion collisions.

The jet angular correlations were measured in $\sqrt{s_{\text{NN}}} = 2.76$ TeV Pb+Pb collisions using 0.14 nb^{-1} of data recorded in 2011 by the ATLAS detector at the LHC. The measurements were performed using jets reconstructed with the anti- k_t algorithm for jet radii $d = 0.2$, $d = 0.3$, and $d = 0.4$. The production of pairs of correlated jets was quantified using the rate of neighbouring jets that accompany a test jet, $R_{\Delta R}$, evaluated both as a function of test-jet E_T and neighbouring-jet E_T . A significant dependence of $R_{\Delta R}$ on collision centrality is observed in both cases, suggesting a suppression of neighbouring jets which increases with increasing centrality of the collision. The centrality dependence of the suppression was further quantified using the central-to-peripheral ratio of $R_{\Delta R}$ distributions, $\rho_{R_{\Delta R}}$. The trends seen in $\rho_{R_{\Delta R}}$ evaluated as a function of neighbouring-jet E_T indicate a decrease in suppression with increasing neighbouring-jet E_T which is, however, of limited significance due to the limited size of the available data sample. The $\rho_{R_{\Delta R}}$ evaluated as a function of test-jet E_T exhibits a suppression reaching values of 0.5–0.7 in 0–10% central collisions and does not show any strong dependence on E_T . This behaviour of the neighbouring jet production can be used to constrain the theoretical models aiming to describe fluctuations in the jet energy loss.

Acknowledgements

We thank CERN for the very successful operation of the LHC, as well as the support staff from our institutions without whom ATLAS could not be operated efficiently.

We acknowledge the support of ANPCyT, Argentina; YerPhI, Armenia; ARC, Australia; BMWFW and FWF, Austria; ANAS, Azerbaijan; SSTC, Belarus; CNPq and FAPESP, Brazil; NSERC, NRC and CFI, Canada; CERN; CONICYT, Chile; CAS, MOST and NSFC, China; COLCIENCIAS, Colombia; MSMT CR, MPO CR and VSC CR, Czech Republic; DNRF, DNSRC and Lundbeck Foundation, Denmark; IN2P3-CNRS, CEA-DSM/IRFU, France; GNSF, Georgia; BMBF, HGF, and MPG, Germany; GSRT, Greece; RGC, Hong Kong SAR, China; ISF,

I-CORE and Benoziyo Center, Israel; INFN, Italy; MEXT and JSPS, Japan; CNRST, Morocco; FOM and NWO, Netherlands; RCN, Norway; MNiSW and NCN, Poland; FCT, Portugal; MNE/IFA, Romania; MES of Russia and NRC KI, Russian Federation; JINR; MESTD, Serbia; MSSR, Slovakia; ARRS and MIZŠ, Slovenia; DST/NRF, South Africa; MINECO, Spain; SRC and Wallenberg Foundation, Sweden; SERI, SNSF and Cantons of Bern and Geneva, Switzerland; MOST, Taiwan; TAEK, Turkey; STFC, United Kingdom; DOE and NSF, United States of America. In addition, individual groups and members have received support from BCKDF, the Canada Council, CANARIE, CRC, Compute Canada, FQRNT, and the Ontario Innovation Trust, Canada; EPLANET, ERC, FP7, Horizon 2020 and Marie Skłodowska-Curie Actions, European Union; Investissements d'Avenir Labex and Idex, ANR, Region Auvergne and Fondation Partager le Savoir, France; DFG and AvH Foundation, Germany; Herakleitos, Thales and Aristeia programmes co-financed by EU-ESF and the Greek NSRF; BSF, GIF and Minerva, Israel; BRF, Norway; the Royal Society and Leverhulme Trust, United Kingdom.

The crucial computing support from all WLCG partners is acknowledged gratefully, in particular from CERN and the ATLAS Tier-1 facilities at TRIUMF (Canada), NDGF (Denmark, Norway, Sweden), CC-IN2P3 (France), KIT/GridKA (Germany), INFN-CNAF (Italy), NL-T1 (Netherlands), PIC (Spain), ASGC (Taiwan), RAL (UK) and BNL (USA) and in the Tier-2 facilities worldwide.

References

- [1] A. Majumder, M. Van Leeuwen, *Prog. Part. Nucl. Phys.* A 66 (2011) 41–92, arXiv:1002.2206.
- [2] ATLAS Collaboration, *Phys. Rev. Lett.* 105 (2010) 252303, arXiv:1011.6182.
- [3] CMS Collaboration, *Phys. Rev. C* 84 (2011) 024906, arXiv:1102.1957.
- [4] ATLAS Collaboration, *Phys. Lett. B* 719 (2013) 220–241, arXiv:1208.1967.
- [5] ATLAS Collaboration, *Phys. Rev. Lett.* 114 (7) (2015) 072302, arXiv:1411.2357.
- [6] ATLAS Collaboration, *Phys. Rev. Lett.* 111 (2013) 152301, arXiv:1306.6469.
- [7] V.M. Abazov, et al., DØ Collaboration, *Phys. Lett. B* 718 (2012) 56–63, arXiv:1207.4957.
- [8] M. Cacciari, G.P. Salam, G. Soyez, *J. High Energy Phys.* 04 (2008) 063, arXiv:0802.1189.
- [9] ATLAS Collaboration, *J. Instrum.* 3 (2008) S08003.
- [10] ATLAS Collaboration, *J. High Energy Phys.* 09 (2010) 056, arXiv:1005.5254.
- [11] ATLAS Collaboration, *Phys. Lett. B* 707 (2012) 330–348, arXiv:1108.6018.
- [12] T. Sjöstrand, S. Mrenna, P.Z. Skands, *J. High Energy Phys.* 05 (2006) 026, arXiv:hep-ph/0603175.
- [13] ATLAS Collaboration, ATL-PHYS-PUB-2011-009, <https://cdsweb.cern.ch/record/1363300>.
- [14] S. Agostinelli, et al., GEANT4 Collaboration, *Nucl. Instrum. Methods A* 506 (2003) 250–303.
- [15] ATLAS Collaboration, *Eur. Phys. J. C* 70 (2010) 823–874, <http://dx.doi.org/10.1140/epjc/s10052-010-1429-9>, arXiv:1005.4568.
- [16] ATLAS Collaboration, *Eur. Phys. J. C* 73 (2013) 2304, arXiv:1112.6426.
- [17] ATLAS Collaboration, ATLAS-CONF-2015-016, <https://cds.cern.ch/record/2008677>.
- [18] I. Lokhtin, A. Snigirev, *Eur. Phys. J. C* 45 (2006) 211–217, arXiv:hep-ph/0506189.
- [19] A. Buckley, H. Hoeth, H. Lacker, H. Schulz, J.E. von Seggern, *Eur. Phys. J. C* 65 (2010) 331–357, <http://dx.doi.org/10.1140/epjc/s10052-009-1196-7>, arXiv:0907.2973.
- [20] ATLAS Collaboration, *Phys. Lett. B* 739 (2014) 320–342, <http://dx.doi.org/10.1016/j.physletb.2014.10.065>, arXiv:1406.2979.
- [21] CMS Collaboration, *J. High Energy Phys.* 10 (2012) 087, arXiv:1205.5872.

ATLAS Collaboration

G. Aad⁸⁴, B. Abbott¹¹², J. Abdallah¹⁵², S. Abdel Khalek¹¹⁶, O. Abdinov¹¹, R. Aben¹⁰⁶, B. Abi¹¹³, M. Abolins⁸⁹, O.S. AbouZeid¹⁵⁹, H. Abramowicz¹⁵⁴, H. Abreu¹⁵³, R. Abreu³⁰, Y. Abulaiti^{147a,147b}, B.S. Acharya^{165a,165b,a}, L. Adamczyk^{38a}, D.L. Adams²⁵, J. Adelman¹⁷⁷, S. Adomeit⁹⁹, T. Adye¹³⁰, T. Agatonovic-Jovin¹³, J.A. Aguilar-Saavedra^{125a,125f}, M. Agustoni¹⁷, S.P. Ahlen²², F. Ahmadov^{64,b}, G. Aielli^{134a,134b}, H. Akerstedt^{147a,147b}, T.P.A. Åkesson⁸⁰, G. Akimoto¹⁵⁶, A.V. Akimov⁹⁵,

G.L. Alberghi^{20a,20b}, J. Albert¹⁷⁰, S. Albrand⁵⁵, M.J. Alconada Verzini⁷⁰, M. Aleksa³⁰, I.N. Aleksandrov⁶⁴, C. Alexa^{26a}, G. Alexander¹⁵⁴, G. Alexandre⁴⁹, T. Alexopoulos¹⁰, M. Alhroob^{165a,165c}, G. Alimonti^{90a}, L. Alio⁸⁴, J. Alison³¹, B.M.M. Allbrooke¹⁸, L.J. Allison⁷¹, P.P. Allport⁷³, J. Almond⁸³, A. Aloisio^{103a,103b}, A. Alonso³⁶, F. Alonso⁷⁰, C. Alpigiani⁷⁵, A. Altheimer³⁵, B. Alvarez Gonzalez⁸⁹, M.G. Alviggi^{103a,103b}, K. Amako⁶⁵, Y. Amaral Coutinho^{24a}, C. Amelung²³, D. Amidei⁸⁸, S.P. Amor Dos Santos^{125a,125c}, A. Amorim^{125a,125b}, S. Amoroso⁴⁸, N. Amram¹⁵⁴, G. Amundsen²³, C. Anastopoulos¹⁴⁰, L.S. Ancu⁴⁹, N. Andari³⁰, T. Andeen³⁵, C.F. Anders^{58b}, G. Anders³⁰, K.J. Anderson³¹, A. Andreazza^{90a,90b}, V. Andrei^{58a}, X.S. Anduaga⁷⁰, S. Angelidakis⁹, I. Angelozzi¹⁰⁶, P. Anger⁴⁴, A. Angerami³⁵, F. Anghinolfi³⁰, A.V. Anisenkov^{108,c}, N. Anjos^{125a}, A. Annovi⁴⁷, A. Antonaki⁹, M. Antonelli⁴⁷, A. Antonov⁹⁷, J. Antos^{145b}, F. Anulli^{133a}, M. Aoki⁶⁵, L. Aperio Bella¹⁸, R. Apolle^{119,d}, G. Arabidze⁸⁹, I. Aracena¹⁴⁴, Y. Arai⁶⁵, J.P. Araque^{125a}, A.T.H. Arce⁴⁵, J.-F. Arguin⁹⁴, S. Argyropoulos⁴², M. Arik^{19a}, A.J. Armbruster³⁰, O. Arnaez³⁰, V. Arnal⁸¹, H. Arnold⁴⁸, M. Arratia²⁸, O. Arslan²¹, A. Artamonov⁹⁶, G. Artoni²³, S. Asai¹⁵⁶, N. Asbah⁴², A. Ashkenazi¹⁵⁴, B. Åsman^{147a,147b}, L. Asquith⁶, K. Assamagan²⁵, R. Astalos^{145a}, M. Atkinson¹⁶⁶, N.B. Atlay¹⁴², B. Auerbach⁶, K. Augsten¹²⁷, M. Auresseau^{146b}, G. Avolio³⁰, G. Azuelos^{94,e}, Y. Azuma¹⁵⁶, M.A. Baak³⁰, A.E. Baas^{58a}, C. Bacci^{135a,135b}, H. Bachacou¹³⁷, K. Bachas¹⁵⁵, M. Backes³⁰, M. Backhaus³⁰, J. Backus Mayes¹⁴⁴, E. Badescu^{26a}, P. Bagiacchi^{133a,133b}, P. Bagnaia^{133a,133b}, Y. Bai^{33a}, T. Bain³⁵, J.T. Baines¹³⁰, O.K. Baker¹⁷⁷, P. Balek¹²⁸, F. Balli¹³⁷, E. Banas³⁹, Sw. Banerjee¹⁷⁴, A.A.E. Bannoura¹⁷⁶, V. Bansal¹⁷⁰, H.S. Bansil¹⁸, L. Barak¹⁷³, E.L. Barberio⁸⁷, D. Barberis^{50a,50b}, M. Barbero⁸⁴, T. Barillari¹⁰⁰, M. Barisonzi¹⁷⁶, T. Barklow¹⁴⁴, N. Barlow²⁸, B.M. Barnett¹³⁰, R.M. Barnett¹⁵, Z. Barnovska⁵, A. Baroncelli^{135a}, G. Barone⁴⁹, A.J. Barr¹¹⁹, F. Barreiro⁸¹, J. Barreiro Guimarães da Costa⁵⁷, R. Bartoldus¹⁴⁴, A.E. Barton⁷¹, P. Bartos^{145a}, V. Bartsch¹⁵⁰, A. Bassalat¹¹⁶, A. Basye¹⁶⁶, R.L. Bates⁵³, J.R. Batley²⁸, M. Battaglia¹³⁸, M. Battistin³⁰, F. Bauer¹³⁷, H.S. Bawa^{144,f}, M.D. Beattie⁷¹, T. Beau⁷⁹, P.H. Beauchemin¹⁶², R. Beccherle^{123a,123b}, P. Bechtel²¹, H.P. Beck^{17,g}, K. Becker¹⁷⁶, S. Becker⁹⁹, M. Beckingham¹⁷¹, C. Becot¹¹⁶, A.J. Beddall^{19c}, A. Beddall^{19c}, S. Bedikian¹⁷⁷, V.A. Bednyakov⁶⁴, C.P. Bee¹⁴⁹, L.J. Beemster¹⁰⁶, T.A. Beermann¹⁷⁶, M. Begel²⁵, J.K. Behr¹¹⁹, C. Belanger-Champagne⁸⁶, P.J. Bell⁴⁹, W.H. Bell⁴⁹, G. Bella¹⁵⁴, L. Bellagamba^{20a}, A. Bellerive²⁹, M. Bellomo⁸⁵, K. Belotskiy⁹⁷, O. Beltramello³⁰, O. Benary¹⁵⁴, D. Bencheekroun^{136a}, K. Bendtz^{147a,147b}, N. Benekos¹⁶⁶, Y. Benhammou¹⁵⁴, E. Benhar Noccioli⁴⁹, J.A. Benitez Garcia^{160b}, D.P. Benjamin⁴⁵, J.R. Bensinger²³, K. Benslama¹³¹, S. Bentvelsen¹⁰⁶, D. Berge¹⁰⁶, E. Bergeaas Kuutmann¹⁶⁷, N. Berger⁵, F. Berghaus¹⁷⁰, J. Beringer¹⁵, C. Bernard²², P. Bernat⁷⁷, C. Bernius⁷⁸, F.U. Bernlochner¹⁷⁰, T. Berry⁷⁶, P. Berta¹²⁸, C. Bertella⁸⁴, G. Bertoli^{147a,147b}, F. Bertolucci^{123a,123b}, C. Bertsche¹¹², D. Bertsche¹¹², M.I. Besana^{90a}, G.J. Besjes¹⁰⁵, O. Bessidskaia Bylund^{147a,147b}, M. Bessner⁴², N. Besson¹³⁷, C. Betancourt⁴⁸, S. Bethke¹⁰⁰, W. Bhimji⁴⁶, R.M. Bianchi¹²⁴, L. Bianchini²³, M. Bianco³⁰, O. Biebel⁹⁹, S.P. Bieniek⁷⁷, K. Bierwagen⁵⁴, J. Biesiada¹⁵, M. Biglietti^{135a}, J. Bilbao De Mendizabal⁴⁹, H. Bilokon⁴⁷, M. Bindi⁵⁴, S. Binet¹¹⁶, A. Bingul^{19c}, C. Bini^{133a,133b}, C.W. Black¹⁵¹, J.E. Black¹⁴⁴, K.M. Black²², D. Blackburn¹³⁹, R.E. Blair⁶, J.-B. Blanchard¹³⁷, T. Blazek^{145a}, I. Bloch⁴², C. Blocker²³, W. Blum^{82,*}, U. Blumenschein⁵⁴, G.J. Bobbink¹⁰⁶, V.S. Bobrovnikov^{108,c}, S.S. Bocchetta⁸⁰, A. Bocci⁴⁵, C. Bock⁹⁹, C.R. Boddy¹¹⁹, M. Boehler⁴⁸, T.T. Boek¹⁷⁶, J.A. Bogaerts³⁰, A.G. Bogdanchikov¹⁰⁸, A. Bogouch^{91,*}, C. Bohm^{147a}, J. Bohm¹²⁶, V. Boisvert⁷⁶, T. Bold^{38a}, V. Boldea^{26a}, A.S. Boldyrev⁹⁸, M. Bomben⁷⁹, M. Bona⁷⁵, M. Boonekamp¹³⁷, A. Borisov¹²⁹, G. Borissov⁷¹, M. Borri⁸³, S. Borroni⁴², J. Bortfeldt⁹⁹, V. Bortolotto^{135a,135b}, K. Bos¹⁰⁶, D. Boscherini^{20a}, M. Bosman¹², H. Boterenbrood¹⁰⁶, J. Boudreau¹²⁴, J. Bouffard², E.V. Bouhova-Thacker⁷¹, D. Boumediene³⁴, C. Bourdarios¹¹⁶, N. Bousson¹¹³, S. Boutouil^{136d}, A. Boveia³¹, J. Boyd³⁰, I.R. Boyko⁶⁴, J. Bracinik¹⁸, A. Brandt⁸, G. Brandt¹⁵, O. Brandt^{58a}, U. Bratzler¹⁵⁷, B. Brau⁸⁵, J.E. Brau¹¹⁵, H.M. Braun^{176,*}, S.F. Brazzale^{165a,165c}, B. Brelier¹⁵⁹, K. Brendlinger¹²¹, A.J. Brennan⁸⁷, R. Brenner¹⁶⁷, S. Bressler¹⁷³, K. Bristow^{146c}, T.M. Bristow⁴⁶, D. Britton⁵³, F.M. Brochu²⁸, I. Brock²¹, R. Brock⁸⁹, C. Bromberg⁸⁹, J. Bronner¹⁰⁰, G. Brooijmans³⁵, T. Brooks⁷⁶, W.K. Brooks^{32b}, J. Brosamer¹⁵, E. Brost¹¹⁵, J. Brown⁵⁵, P.A. Bruckman de Renstrom³⁹, D. Bruncko^{145b}, R. Bruneliere⁴⁸, S. Brunet⁶⁰, A. Bruni^{20a}, G. Bruni^{20a}, M. Bruschi^{20a}, L. Bryngemark⁸⁰, T. Buanes¹⁴, Q. Buat¹⁴³, F. Bucci⁴⁹, P. Buchholz¹⁴², R.M. Buckingham¹¹⁹, A.G. Buckley⁵³, S.I. Buda^{26a}, I.A. Budagov⁶⁴, F. Buehrer⁴⁸, L. Bugge¹¹⁸, M.K. Bugge¹¹⁸, O. Bulekov⁹⁷, A.C. Bundock⁷³, H. Burckhart³⁰, S. Burdin⁷³, B. Burghgrave¹⁰⁷, S. Burke¹³⁰, I. Burmeister⁴³, E. Busato³⁴, D. Büscher⁴⁸, V. Büscher⁸²,

P. Bussey⁵³, C.P. Buszello¹⁶⁷, B. Butler⁵⁷, J.M. Butler²², A.I. Butt³, C.M. Buttar⁵³, J.M. Butterworth⁷⁷, P. Butti¹⁰⁶, W. Buttinger²⁸, A. Buzatu⁵³, M. Byszewski¹⁰, S. Cabrera Urbán¹⁶⁸, D. Caforio^{20a,20b}, O. Cakir^{4a}, P. Calafiura¹⁵, A. Calandri¹³⁷, G. Calderini⁷⁹, P. Calfayan⁹⁹, R. Calkins¹⁰⁷, L.P. Caloba^{24a}, D. Calvet³⁴, S. Calvet³⁴, R. Camacho Toro⁴⁹, S. Camarda⁴², D. Cameron¹¹⁸, L.M. Caminada¹⁵, R. Caminal Armadans¹², S. Campana³⁰, M. Campanelli⁷⁷, A. Campoverde¹⁴⁹, V. Canale^{103a,103b}, A. Canepa^{160a}, M. Cano Bret⁷⁵, J. Cantero⁸¹, R. Cantrill^{125a}, T. Cao⁴⁰, M.D.M. Capeans Garrido³⁰, I. Caprini^{26a}, M. Caprini^{26a}, M. Capua^{37a,37b}, R. Caputo⁸², R. Cardarelli^{134a}, T. Carli³⁰, G. Carlino^{103a}, L. Carminati^{90a,90b}, S. Caron¹⁰⁵, E. Carquin^{32a}, G.D. Carrillo-Montoya^{146c}, J.R. Carter²⁸, J. Carvalho^{125a,125c}, D. Casadei⁷⁷, M.P. Casado¹², M. Casolino¹², E. Castaneda-Miranda^{146b}, A. Castelli¹⁰⁶, V. Castillo Gimenez¹⁶⁸, N.F. Castro^{125a,h}, P. Catastini⁵⁷, A. Catinaccio³⁰, J.R. Catmore¹¹⁸, A. Cattai³⁰, G. Cattani^{134a,134b}, J. Caudron⁸², S. Caughron⁸⁹, V. Cavaliere¹⁶⁶, D. Cavalli^{90a}, M. Cavalli-Sforza¹², V. Cavasinni^{123a,123b}, F. Ceradini^{135a,135b}, B.C. Cerio⁴⁵, K. Cerny¹²⁸, A.S. Cerqueira^{24b}, A. Cerri¹⁵⁰, L. Cerrito⁷⁵, F. Cerutti¹⁵, M. Cerv³⁰, A. Cervelli¹⁷, S.A. Cetin^{19b}, A. Chafaq^{136a}, D. Chakraborty¹⁰⁷, I. Chalupkova¹²⁸, P. Chang¹⁶⁶, B. Chapleau⁸⁶, J.D. Chapman²⁸, D. Charfeddine¹¹⁶, D.G. Charlton¹⁸, C.C. Chau¹⁵⁹, C.A. Chavez Barajas¹⁵⁰, S. Cheatham⁸⁶, A. Chegwidden⁸⁹, S. Chekanov⁶, S.V. Chekulaev^{160a}, G.A. Chelkov^{64,i}, M.A. Chelstowska⁸⁸, C. Chen⁶³, H. Chen²⁵, K. Chen¹⁴⁹, L. Chen^{33d,j}, S. Chen^{33c}, X. Chen^{146c}, Y. Chen⁶⁶, Y. Chen³⁵, H.C. Cheng⁸⁸, Y. Cheng³¹, A. Cheplakov⁶⁴, R. Cherkaoui El Moursli^{136e}, V. Chernyatin^{25,*}, E. Cheu⁷, L. Chevalier¹³⁷, V. Chiarella⁴⁷, G. Chiefari^{103a,103b}, J.T. Childers⁶, A. Chilingarov⁷¹, G. Chiodini^{72a}, A.S. Chisholm¹⁸, R.T. Chislett⁷⁷, A. Chitan^{26a}, M.V. Chizhov⁶⁴, S. Chouridou⁹, B.K.B. Chow⁹⁹, D. Chromek-Burckhart³⁰, M.L. Chu¹⁵², J. Chudoba¹²⁶, J.J. Chwastowski³⁹, L. Chytka¹¹⁴, G. Ciapetti^{133a,133b}, A.K. Ciftci^{4a}, R. Ciftci^{4a}, D. Cinca⁵³, V. Cindro⁷⁴, A. Ciocio¹⁵, P. Cirkovic¹³, Z.H. Citron¹⁷³, M. Ciubancan^{26a}, A. Clark⁴⁹, P.J. Clark⁴⁶, R.N. Clarke¹⁵, W. Cleland¹²⁴, J.C. Clemens⁸⁴, C. Clement^{147a,147b}, Y. Coadou⁸⁴, M. Cobal^{165a,165c}, A. Coccaro¹³⁹, J. Cochran⁶³, L. Coffey²³, J.G. Cogan¹⁴⁴, J. Coggeshall¹⁶⁶, B. Cole³⁵, S. Cole¹⁰⁷, A.P. Colijn¹⁰⁶, J. Collot⁵⁵, T. Colombo^{58c}, G. Colon⁸⁵, G. Compostella¹⁰⁰, P. Conde Muiño^{125a,125b}, E. Coniavitis⁴⁸, M.C. Conidi¹², S.H. Connell^{146b}, I.A. Connelly⁷⁶, S.M. Consonni^{90a,90b}, V. Consorti⁴⁸, S. Constantinescu^{26a}, C. Conta^{120a,120b}, G. Conti⁵⁷, F. Conventi^{103a,k}, M. Cooke¹⁵, B.D. Cooper⁷⁷, A.M. Cooper-Sarkar¹¹⁹, N.J. Cooper-Smith⁷⁶, K. Copic¹⁵, T. Cornelissen¹⁷⁶, M. Corradi^{20a}, F. Corriveau^{86,l}, A. Corso-Radu¹⁶⁴, A. Cortes-Gonzalez¹², G. Cortiana¹⁰⁰, G. Costa^{90a}, M.J. Costa¹⁶⁸, D. Costanzo¹⁴⁰, D. Côté⁸, G. Cottin²⁸, G. Cowan⁷⁶, B.E. Cox⁸³, K. Cranmer¹⁰⁹, G. Cree²⁹, S. Crépé-Renaudin⁵⁵, F. Crescioli⁷⁹, W.A. Cribbs^{147a,147b}, M. Crispin Ortuzar¹¹⁹, M. Cristinziani²¹, V. Croft¹⁰⁵, G. Crosetti^{37a,37b}, C.-M. Cuciuc^{26a}, T. Cuhadar Donszelmann¹⁴⁰, J. Cummings¹⁷⁷, M. Curatolo⁴⁷, C. Cuthbert¹⁵¹, H. Czirr¹⁴², P. Czodrowski³, Z. Czyzula¹⁷⁷, S. D'Auria⁵³, M. D'Onofrio⁷³, M.J. Da Cunha Sargedas De Sousa^{125a,125b}, C. Da Via⁸³, W. Dabrowski^{38a}, A. Dafinca¹¹⁹, T. Dai⁸⁸, O. Dale¹⁴, F. Dallaire⁹⁴, C. Dallapiccola⁸⁵, M. Dam³⁶, A.C. Daniells¹⁸, M. Dano Hoffmann¹³⁷, V. Dao⁴⁸, G. Darbo^{50a}, S. Darmora⁸, J. Dassoulas⁴², A. Dattagupta⁶⁰, W. Davey²¹, C. David¹⁷⁰, T. Davidek¹²⁸, E. Davies^{119,d}, M. Davies¹⁵⁴, O. Davignon⁷⁹, A.R. Davison⁷⁷, P. Davison⁷⁷, Y. Davygora^{58a}, E. Dawe¹⁴³, I. Dawson¹⁴⁰, R.K. Daya-Ishmukhametova⁸⁵, K. De⁸, R. de Asmundis^{103a}, S. De Castro^{20a,20b}, S. De Cecco⁷⁹, N. De Groot¹⁰⁵, P. de Jong¹⁰⁶, H. De la Torre⁸¹, F. De Lorenzi⁶³, L. De Nooij¹⁰⁶, D. De Pedis^{133a}, A. De Salvo^{133a}, U. De Sanctis^{165a,165b}, A. De Santo¹⁵⁰, J.B. De Vivie De Regie¹¹⁶, W.J. Dearnaley⁷¹, R. Debbe²⁵, C. Debenedetti¹³⁸, B. Dechenaux⁵⁵, D.V. Dedovich⁶⁴, I. Deigaard¹⁰⁶, J. Del Peso⁸¹, T. Del Prete^{123a,123b}, F. Deliot¹³⁷, C.M. Delitzsch⁴⁹, M. Deliyergiyev⁷⁴, A. Dell'Acqua³⁰, L. Dell'Asta²², M. Dell'Orso^{123a,123b}, M. Della Pietra^{103a,k}, D. della Volpe⁴⁹, M. Delmastro⁵, P.A. Delsart⁵⁵, C. Deluca¹⁰⁶, S. Demers¹⁷⁷, M. Demichev⁶⁴, A. Demilly⁷⁹, S.P. Denisov¹²⁹, D. Derendarz³⁹, J.E. Derkaoui^{136d}, F. Derue⁷⁹, P. Dervan⁷³, K. Desch²¹, C. Deterre⁴², P.O. Deviveiros¹⁰⁶, A. Dewhurst¹³⁰, S. Dhaliwal¹⁰⁶, A. Di Ciaccio^{134a,134b}, L. Di Ciaccio⁵, A. Di Domenico^{133a,133b}, C. Di Donato^{103a,103b}, A. Di Girolamo³⁰, B. Di Girolamo³⁰, A. Di Mattia¹⁵³, B. Di Micco^{135a,135b}, R. Di Nardo⁴⁷, A. Di Simone⁴⁸, R. Di Sipio^{20a,20b}, D. Di Valentino²⁹, F.A. Dias⁴⁶, M.A. Diaz^{32a}, E.B. Diehl⁸⁸, J. Dietrich⁴², T.A. Dietzsch^{58a}, S. Diglio⁸⁴, A. Dimitrievska¹³, J. Dingfelder²¹, C. Dionisi^{133a,133b}, P. Dita^{26a}, S. Dita^{26a}, F. Dittus³⁰, F. Djama⁸⁴, T. Djobava^{51b}, J.I. Djuvsland^{58a}, M.A.B. do Vale^{24c}, A. Do Valle Wemans^{125a,125g}, T.K.O. Doan⁵, D. Dobos³⁰, C. Doglioni⁴⁹, T. Doherty⁵³, T. Dohmae¹⁵⁶, J. Dolejsi¹²⁸, Z. Dolezal¹²⁸, B.A. Dolgoshein^{97,*}, M. Donadelli^{24d}, S. Donati^{123a,123b},

P. Dondero ^{120a,120b}, J. Donini ³⁴, J. Dopke ¹³⁰, A. Doria ^{103a}, M.T. Dova ⁷⁰, A.T. Doyle ⁵³, M. Dris ¹⁰, J. Dubbert ⁸⁸, S. Dube ¹⁵, E. Dubreuil ³⁴, E. Duchovni ¹⁷³, G. Duckeck ⁹⁹, O.A. Ducu ^{26a}, D. Duda ¹⁷⁶, A. Dudarev ³⁰, F. Dudziak ⁶³, L. Duflot ¹¹⁶, L. Duguid ⁷⁶, M. Dührssen ³⁰, M. Dunford ^{58a}, H. Duran Yildiz ^{4a}, M. Düren ⁵², A. Durglishvili ^{51b}, M. Dwuznik ^{38a}, M. Dyndal ^{38a}, J. Ebke ⁹⁹, W. Edson ², N.C. Edwards ⁴⁶, W. Ehrenfeld ²¹, T. Eifert ¹⁴⁴, G. Eigen ¹⁴, K. Einsweiler ¹⁵, T. Ekelof ¹⁶⁷, M. El Kacimi ^{136c}, M. Ellert ¹⁶⁷, S. Elles ⁵, F. Ellinghaus ⁸², N. Ellis ³⁰, J. Elmsheuser ⁹⁹, M. Elsing ³⁰, D. Emelianov ¹³⁰, Y. Enari ¹⁵⁶, O.C. Endner ⁸², M. Endo ¹¹⁷, J. Erdmann ¹⁷⁷, A. Ereditato ¹⁷, D. Eriksson ^{147a}, G. Ernis ¹⁷⁶, J. Ernst ², M. Ernst ²⁵, J. Ernwein ¹³⁷, D. Errede ¹⁶⁶, S. Errede ¹⁶⁶, E. Ertel ⁸², M. Escalier ¹¹⁶, H. Esch ⁴³, C. Escobar ¹²⁴, B. Esposito ⁴⁷, A.I. Etiennevre ¹³⁷, E. Etzion ¹⁵⁴, H. Evans ⁶⁰, A. Ezhilov ¹²², L. Fabbri ^{20a,20b}, G. Facini ³¹, R.M. Fakhruddinov ¹²⁹, S. Falciano ^{133a}, R.J. Falla ⁷⁷, J. Faltova ¹²⁸, Y. Fang ^{33a}, M. Fanti ^{90a,90b}, A. Farbin ⁸, A. Farilla ^{135a}, T. Farooque ¹², S. Farrell ¹⁵, S.M. Farrington ¹⁷¹, P. Farthouat ³⁰, F. Fassi ^{136e}, P. Fassnacht ³⁰, D. Fassoulitis ⁹, A. Favareto ^{50a,50b}, L. Fayard ¹¹⁶, P. Federic ^{145a}, O.L. Fedin ^{122,m}, W. Fedorko ¹⁶⁹, M. Fehling-Kaschek ⁴⁸, S. Feigl ³⁰, L. Feligioni ⁸⁴, C. Feng ^{33d}, E.J. Feng ⁶, H. Feng ⁸⁸, A.B. Fenyuk ¹²⁹, S. Fernandez Perez ³⁰, S. Ferrag ⁵³, J. Ferrando ⁵³, A. Ferrari ¹⁶⁷, P. Ferrari ¹⁰⁶, R. Ferrari ^{120a}, D.E. Ferreira de Lima ⁵³, A. Ferrer ¹⁶⁸, D. Ferrere ⁴⁹, C. Ferretti ⁸⁸, A. Ferretto Parodi ^{50a,50b}, M. Fiascaris ³¹, F. Fiedler ⁸², A. Filipčič ⁷⁴, M. Filipuzzi ⁴², F. Filthaut ¹⁰⁵, M. Fincke-Keeler ¹⁷⁰, K.D. Finelli ¹⁵¹, M.C.N. Fiolhais ^{125a,125c}, L. Fiorini ¹⁶⁸, A. Firan ⁴⁰, A. Fischer ², J. Fischer ¹⁷⁶, W.C. Fisher ⁸⁹, E.A. Fitzgerald ²³, M. Flechl ⁴⁸, I. Fleck ¹⁴², P. Fleischmann ⁸⁸, S. Fleischmann ¹⁷⁶, G.T. Fletcher ¹⁴⁰, G. Fletcher ⁷⁵, T. Flick ¹⁷⁶, A. Floderus ⁸⁰, L.R. Flores Castillo ^{174,n}, A.C. Florez Bustos ^{160b}, M.J. Flowerdew ¹⁰⁰, A. Formica ¹³⁷, A. Forti ⁸³, D. Fortin ^{160a}, D. Fournier ¹¹⁶, H. Fox ⁷¹, S. Fracchia ¹², P. Francavilla ⁷⁹, M. Franchini ^{20a,20b}, S. Franchino ³⁰, D. Francis ³⁰, L. Franconi ¹¹⁸, M. Franklin ⁵⁷, S. Franz ⁶¹, M. Fraternali ^{120a,120b}, S.T. French ²⁸, C. Friedrich ⁴², F. Friedrich ⁴⁴, D. Froidevaux ³⁰, J.A. Frost ²⁸, C. Fukunaga ¹⁵⁷, E. Fullana Torregrosa ⁸², B.G. Fulsom ¹⁴⁴, J. Fuster ¹⁶⁸, C. Gabaldon ⁵⁵, O. Gabizon ¹⁷³, A. Gabrielli ^{20a,20b}, A. Gabrielli ^{133a,133b}, S. Gadatsch ¹⁰⁶, S. Gadomski ⁴⁹, G. Gagliardi ^{50a,50b}, P. Gagnon ⁶⁰, C. Galea ¹⁰⁵, B. Galhardo ^{125a,125c}, E.J. Gallas ¹¹⁹, V. Gallo ¹⁷, B.J. Gallop ¹³⁰, P. Gallus ¹²⁷, G. Galster ³⁶, K.K. Gan ¹¹⁰, R.P. Gandrajula ⁶², J. Gao ^{33b,84}, Y.S. Gao ^{144,f}, F.M. Garay Walls ⁴⁶, F. Garbersson ¹⁷⁷, C. García ¹⁶⁸, J.E. García Navarro ¹⁶⁸, M. Garcia-Sciveres ¹⁵, R.W. Gardner ³¹, N. Garelli ¹⁴⁴, V. Garonne ³⁰, C. Gatti ⁴⁷, G. Gaudio ^{120a}, B. Gaur ¹⁴², L. Gauthier ⁹⁴, P. Gauzzi ^{133a,133b}, I.L. Gavrilenko ⁹⁵, C. Gay ¹⁶⁹, G. Gaycken ²¹, E.N. Gazis ¹⁰, P. Ge ^{33d}, Z. Gece ¹⁶⁹, C.N.P. Gee ¹³⁰, D.A.A. Geerts ¹⁰⁶, Ch. Geich-Gimbel ²¹, C. Gemme ^{50a}, A. Gemmell ⁵³, M.H. Genest ⁵⁵, S. Gentile ^{133a,133b}, M. George ⁵⁴, S. George ⁷⁶, D. Gerbaudo ¹⁶⁴, A. Gershon ¹⁵⁴, H. Ghazlane ^{136b}, N. Ghodbane ³⁴, B. Giacobbe ^{20a}, S. Giagu ^{133a,133b}, V. Giangiobbe ¹², P. Giannetti ^{123a,123b}, F. Gianotti ³⁰, B. Gibbard ²⁵, S.M. Gibson ⁷⁶, M. Gilchriese ¹⁵, T.P.S. Gillam ²⁸, D. Gillberg ³⁰, G. Gilles ³⁴, D.M. Gingrich ^{3,e}, N. Giokaris ⁹, M.P. Giordani ^{165a,165c}, R. Giordano ^{103a,103b}, F.M. Giorgi ^{20a}, F.M. Giorgi ¹⁶, P.F. Giraud ¹³⁷, D. Giugni ^{90a}, C. Giuliani ⁴⁸, M. Giulini ^{58b}, B.K. Gjelsten ¹¹⁸, S. Gkaitatzis ¹⁵⁵, I. Gkialas ¹⁵⁵, L.K. Gladilin ⁹⁸, C. Glasman ⁸¹, J. Glatzer ³⁰, P.C.F. Glaysheer ⁴⁶, A. Glazov ⁴², G.L. Glonti ⁶⁴, M. Goblirsch-Kolb ¹⁰⁰, J.R. Goddard ⁷⁵, J. Godfrey ¹⁴³, J. Godlewski ³⁰, C. Goeringer ⁸², S. Goldfarb ⁸⁸, T. Golling ¹⁷⁷, D. Golubkov ¹²⁹, A. Gomes ^{125a,125b,125d}, L.S. Gomez Fajardo ⁴², R. Gonçalo ^{125a}, J. Goncalves Pinto Firmino Da Costa ¹³⁷, L. Gonella ²¹, S. González de la Hoz ¹⁶⁸, G. Gonzalez Parra ¹², S. Gonzalez-Sevilla ⁴⁹, L. Goossens ³⁰, P.A. Gorbounov ⁹⁶, H.A. Gordon ²⁵, I. Gorelov ¹⁰⁴, B. Gorini ³⁰, E. Gorini ^{72a,72b}, A. Gorišek ⁷⁴, E. Gornicki ³⁹, A.T. Goshaw ⁶, C. Gössling ⁴³, M.I. Gostkin ⁶⁴, M. Gouighri ^{136a}, D. Goujdami ^{136c}, M.P. Goulette ⁴⁹, A.G. Goussiou ¹³⁹, C. Goy ⁵, S. Gozpinar ²³, H.M.X. Grabas ¹³⁷, L. Graber ⁵⁴, I. Grabowska-Bold ^{38a}, P. Grafström ^{20a,20b}, K-J. Grahn ⁴², J. Gramling ⁴⁹, E. Gramstad ¹¹⁸, S. Grancagnolo ¹⁶, V. Grassi ¹⁴⁹, V. Gratchev ¹²², H.M. Gray ³⁰, E. Graziani ^{135a}, O.G. Grebenyuk ¹²², Z.D. Greenwood ^{78,o}, K. Gregersen ⁷⁷, I.M. Gregor ⁴², P. Grenier ¹⁴⁴, J. Griffiths ⁸, A.A. Grillo ¹³⁸, K. Grimm ⁷¹, S. Grinstein ^{12,p}, Ph. Gris ³⁴, Y.V. Grishkevich ⁹⁸, J.-F. Grivaz ¹¹⁶, J.P. Grohs ⁴⁴, A. Grohsjean ⁴², E. Gross ¹⁷³, J. Grosse-Knetter ⁵⁴, G.C. Grossi ^{134a,134b}, J. Groth-Jensen ¹⁷³, Z.J. Grout ¹⁵⁰, L. Guan ^{33b}, J. Guenther ¹²⁷, F. Guescini ⁴⁹, D. Guest ¹⁷⁷, O. Gueta ¹⁵⁴, C. Guicheney ³⁴, E. Guido ^{50a,50b}, T. Guillemin ¹¹⁶, S. Guindon ², U. Gul ⁵³, C. Gumpert ⁴⁴, J. Guo ³⁵, S. Gupta ¹¹⁹, P. Gutierrez ¹¹², N.G. Gutierrez Ortiz ⁵³, C. Gutsche ⁷⁷, N. Guttman ¹⁵⁴, C. Guyot ¹³⁷, C. Gwenlan ¹¹⁹, C.B. Gwilliam ⁷³, A. Haas ¹⁰⁹, C. Haber ¹⁵, H.K. Hadavand ⁸, N. Haddad ^{136e}, P. Haefner ²¹, S. Hageböck ²¹, Z. Hajduk ³⁹, H. Hakobyan ¹⁷⁸, M. Haleem ⁴², D. Hall ¹¹⁹, G. Halladjian ⁸⁹, K. Hamacher ¹⁷⁶, P. Hamal ¹¹⁴, K. Hamano ¹⁷⁰,

M. Hamer⁵⁴, A. Hamilton^{146a}, S. Hamilton¹⁶², G.N. Hamity^{146c}, P.G. Hamnett⁴², L. Han^{33b}, K. Hanagaki¹¹⁷, K. Hanawa¹⁵⁶, M. Hance¹⁵, P. Hanke^{58a}, R. Hanna¹³⁷, J.B. Hansen³⁶, J.D. Hansen³⁶, P.H. Hansen³⁶, K. Hara¹⁶¹, A.S. Hard¹⁷⁴, T. Harenberg¹⁷⁶, F. Hariri¹¹⁶, S. Harkusha⁹¹, D. Harper⁸⁸, R.D. Harrington⁴⁶, O.M. Harris¹³⁹, P.F. Harrison¹⁷¹, F. Hartjes¹⁰⁶, M. Hasegawa⁶⁶, S. Hasegawa¹⁰², Y. Hasegawa¹⁴¹, A. Hasib¹¹², S. Hassani¹³⁷, S. Haug¹⁷, M. Hauschild³⁰, R. Hauser⁸⁹, M. Havranek¹²⁶, C.M. Hawkes¹⁸, R.J. Hawking³⁰, A.D. Hawkins⁸⁰, T. Hayashi¹⁶¹, D. Hayden⁸⁹, C.P. Hays¹¹⁹, H.S. Hayward⁷³, S.J. Haywood¹³⁰, S.J. Head¹⁸, T. Heck⁸², V. Hedberg⁸⁰, L. Heelan⁸, S. Heim¹²¹, T. Heim¹⁷⁶, B. Heinemann¹⁵, L. Heinrich¹⁰⁹, J. Hejbal¹²⁶, L. Helary²², C. Heller⁹⁹, M. Heller³⁰, S. Hellman^{147a,147b}, D. Hellmich²¹, C. Helsens³⁰, J. Henderson¹¹⁹, R.C.W. Henderson⁷¹, Y. Heng¹⁷⁴, C. Hengler⁴², A. Henrichs¹⁷⁷, A.M. Henriques Correia³⁰, S. Henrot-Versille¹¹⁶, C. Hensel⁵⁴, G.H. Herbert¹⁶, Y. Hernández Jiménez¹⁶⁸, R. Herrberg-Schubert¹⁶, G. Herten⁴⁸, R. Hertenberger⁹⁹, L. Hervas³⁰, G.G. Hesketh⁷⁷, N.P. Hessey¹⁰⁶, R. Hickling⁷⁵, E. Higón-Rodríguez¹⁶⁸, E. Hill¹⁷⁰, J.C. Hill²⁸, K.H. Hiller⁴², S. Hillert²¹, S.J. Hillier¹⁸, I. Hinchliffe¹⁵, E. Hines¹²¹, M. Hirose¹⁵⁸, D. Hirschbuehl¹⁷⁶, J. Hobbs¹⁴⁹, N. Hod¹⁰⁶, M.C. Hodgkinson¹⁴⁰, P. Hodgson¹⁴⁰, A. Hoecker³⁰, M.R. Hoefkamp¹⁰⁴, F. Hoenig⁹⁹, J. Hoffman⁴⁰, D. Hoffmann⁸⁴, M. Hohlfeld⁸², T.R. Holmes¹⁵, T.M. Hong¹²¹, L. Hooft van Huysduynen¹⁰⁹, J.-Y. Hostachy⁵⁵, S. Hou¹⁵², A. Hoummada^{136a}, J. Howard¹¹⁹, J. Howarth⁴², M. Hrabovsky¹¹⁴, I. Hristova¹⁶, J. Hrivnac¹¹⁶, T. Hryn'ova⁵, C. Hsu^{146c}, P.J. Hsu⁸², S.-C. Hsu¹³⁹, D. Hu³⁵, X. Hu⁸⁸, Y. Huang⁴², Z. Hubacek³⁰, F. Hubaut⁸⁴, F. Huegging²¹, T.B. Huffman¹¹⁹, E.W. Hughes³⁵, G. Hughes⁷¹, M. Huhtinen³⁰, T.A. Hülsing⁸², M. Hurwitz¹⁵, N. Huseynov^{64,b}, J. Huston⁸⁹, J. Huth⁵⁷, G. Iacobucci⁴⁹, G. Iakovidis¹⁰, I. Ibragimov¹⁴², L. Iconomidou-Fayard¹¹⁶, E. Ideal¹⁷⁷, P. Iengo^{103a}, O. Igonkina¹⁰⁶, T. Iizawa¹⁷², Y. Ikegami⁶⁵, K. Ikematsu¹⁴², M. Ikeno⁶⁵, Y. Ilchenko^{31,q}, D. Iliadis¹⁵⁵, N. Ilic¹⁵⁹, Y. Inamaru⁶⁶, T. Ince¹⁰⁰, P. Ioannou⁹, M. Iodice^{135a}, K. Iordanidou⁹, V. Ippolito⁵⁷, A. Irles Quiles¹⁶⁸, C. Isaksson¹⁶⁷, M. Ishino⁶⁷, M. Ishitsuka¹⁵⁸, R. Ishmukhametov¹¹⁰, C. Issever¹¹⁹, S. Istin^{19a}, J.M. Iturbe Ponce⁸³, R. Iuppa^{134a,134b}, J. Ivarsson⁸⁰, W. Iwanski³⁹, H. Iwasaki⁶⁵, J.M. Izen⁴¹, V. Izzo^{103a}, B. Jackson¹²¹, M. Jackson⁷³, P. Jackson¹, M.R. Jaekel³⁰, V. Jain², K. Jakobs⁴⁸, S. Jakobsen³⁰, T. Jakoubek¹²⁶, J. Jakubek¹²⁷, D.O. Jamin¹⁵², D.K. Jana⁷⁸, E. Jansen⁷⁷, H. Jansen³⁰, J. Janssen²¹, M. Janus¹⁷¹, G. Jarlskog⁸⁰, N. Javadov^{64,b}, T. Javůrek⁴⁸, L. Jeanty¹⁵, J. Jejelava^{51a,r}, G.-Y. Jeng¹⁵¹, D. Jennens⁸⁷, P. Jenni^{48,s}, J. Jentzsch⁴³, C. Jeske¹⁷¹, S. Jézéquel⁵, H. Ji¹⁷⁴, J. Jia¹⁴⁹, Y. Jiang^{33b}, M. Jimenez Belenguer⁴², S. Jin^{33a}, A. Jinaru^{26a}, O. Jinnouchi¹⁵⁸, M.D. Joergensen³⁶, K.E. Johansson^{147a,147b}, P. Johansson¹⁴⁰, K.A. Johns⁷, K. Jon-And^{147a,147b}, G. Jones¹⁷¹, R.W.L. Jones⁷¹, T.J. Jones⁷³, J. Jongmanns^{58a}, P.M. Jorge^{125a,125b}, K.D. Joshi⁸³, J. Jovicevic¹⁴⁸, X. Ju¹⁷⁴, C.A. Jung⁴³, R.M. Jungst³⁰, P. Jussel⁶¹, A. Juste Rozas^{12,p}, M. Kaci¹⁶⁸, A. Kaczmarska³⁹, M. Kado¹¹⁶, H. Kagan¹¹⁰, M. Kagan¹⁴⁴, E. Kajomovitz⁴⁵, C.W. Kalderon¹¹⁹, S. Kama⁴⁰, A. Kamenshchikov¹²⁹, N. Kanaya¹⁵⁶, M. Kaneda³⁰, S. Kaneti²⁸, V.A. Kantserov⁹⁷, J. Kanzaki⁶⁵, B. Kaplan¹⁰⁹, A. Kapliy³¹, D. Kar⁵³, K. Karakostas¹⁰, N. Karastathis¹⁰, M. Karnevskiy⁸², S.N. Karpov⁶⁴, Z.M. Karpova⁶⁴, K. Karthik¹⁰⁹, V. Kartvelishvili⁷¹, A.N. Karyukhin¹²⁹, L. Kashif¹⁷⁴, G. Kasieczka^{58b}, R.D. Kass¹¹⁰, A. Kastanas¹⁴, Y. Kataoka¹⁵⁶, A. Katre⁴⁹, J. Katzy⁴², V. Kaushik⁷, K. Kawagoe⁶⁹, T. Kawamoto¹⁵⁶, G. Kawamura⁵⁴, S. Kazama¹⁵⁶, V.F. Kazanin^{108,c}, M.Y. Kazarinov⁶⁴, R. Keeler¹⁷⁰, R. Kehoe⁴⁰, J.S. Keller⁴², J.J. Kempster⁷⁶, H. Keoshkerian⁵, O. Kepka¹²⁶, B.P. Kerševan⁷⁴, S. Kersten¹⁷⁶, K. Kessoku¹⁵⁶, J. Keung¹⁵⁹, F. Khalil-zada¹¹, H. Khandanyan^{147a,147b}, A. Khanov¹¹³, A. Khodinov⁹⁷, A. Khomich^{58a}, T.J. Khoo²⁸, G. Khorauli²¹, A. Khoroshilov¹⁷⁶, V. Khovanskiy⁹⁶, E. Khramov⁶⁴, J. Khubua^{51b,t}, H.Y. Kim⁸, H. Kim^{147a,147b}, S.H. Kim¹⁶¹, N. Kimura¹⁷², O.M. Kind¹⁶, B.T. King⁷³, M. King¹⁶⁸, R.S.B. King¹¹⁹, S.B. King¹⁶⁹, J. Kirk¹³⁰, A.E. Kiryunin¹⁰⁰, T. Kishimoto⁶⁶, D. Kisieleska^{38a}, F. Kiss⁴⁸, T. Kittelmann¹²⁴, K. Kiuchi¹⁶¹, E. Kladiva^{145b}, M. Klein⁷³, U. Klein⁷³, K. Kleinknecht⁸², P. Klimek^{147a,147b}, A. Klimentov²⁵, R. Klingenberg⁴³, J.A. Klinger⁸³, T. Klioutchnikova³⁰, P.F. Klok¹⁰⁵, E.-E. Kluge^{58a}, P. Kluit¹⁰⁶, S. Kluth¹⁰⁰, E. Kneringer⁶¹, E.B.F.G. Knoops⁸⁴, A. Knue⁵³, D. Kobayashi¹⁵⁸, T. Kobayashi¹⁵⁶, M. Kobel⁴⁴, M. Kocian¹⁴⁴, P. Kodys¹²⁸, P. Koevesarki²¹, T. Koffas²⁹, E. Koffeman¹⁰⁶, L.A. Kogan¹¹⁹, S. Kohlmann¹⁷⁶, Z. Kohout¹²⁷, T. Kohriki⁶⁵, T. Koi¹⁴⁴, H. Kolanoski¹⁶, I. Koletsou⁵, J. Koll⁸⁹, A.A. Komar^{95,*}, Y. Komori¹⁵⁶, T. Kondo⁶⁵, N. Kondrashova⁴², K. Köneke⁴⁸, A.C. König¹⁰⁵, S. König⁸², T. Kono^{65,u}, R. Konoplich^{109,v}, N. Konstantinidis⁷⁷, R. Kopeliansky¹⁵³, S. Koperny^{38a}, L. Köpke⁸², A.K. Kopp⁴⁸, K. Korcyl³⁹, K. Kordas¹⁵⁵, A. Korn⁷⁷, A.A. Korol^{108,c}, I. Korolkov¹², E.V. Korolkova¹⁴⁰, V.A. Korotkov¹²⁹, O. Kortner¹⁰⁰, S. Kortner¹⁰⁰, V.V. Kostyukhin²¹, V.M. Kotov⁶⁴, A. Kotwal⁴⁵, C. Kourkoumelis⁹,

V. Kouskoura¹⁵⁵, A. Koutsman^{160a}, R. Kowalewski¹⁷⁰, T.Z. Kowalski^{38a}, W. Kozanecki¹³⁷, A.S. Kozhin¹²⁹, V. Kral¹²⁷, V.A. Kramarenko⁹⁸, G. Kramberger⁷⁴, D. Krasnopevtsev⁹⁷, M.W. Krasny⁷⁹, A. Krasznahorkay³⁰, J.K. Kraus²¹, A. Kravchenko²⁵, S. Kreiss¹⁰⁹, M. Kretz^{58c}, J. Kretzschmar⁷³, K. Kreutzfeldt⁵², P. Krieger¹⁵⁹, K. Kroeninger⁵⁴, H. Kroha¹⁰⁰, J. Kroll¹²¹, J. Kroseberg²¹, J. Krstic¹³, U. Kruchonak⁶⁴, H. Krüger²¹, T. Kruker¹⁷, N. Krumnack⁶³, Z.V. Krumshteyn⁶⁴, A. Kruse¹⁷⁴, M.C. Kruse⁴⁵, M. Kruskal²², T. Kubota⁸⁷, S. Kудay^{4a}, S. Kuehn⁴⁸, A. Kugel^{58c}, A. Kuhl¹³⁸, T. Kuhl⁴², V. Kukhtin⁶⁴, Y. Kulchitsky⁹¹, S. Kuleshov^{32b}, M. Kuna^{133a,133b}, J. Kunkle¹²¹, A. Kupco¹²⁶, H. Kurashige⁶⁶, Y.A. Kurochkin⁹¹, R. Kurumida⁶⁶, V. Kus¹²⁶, E.S. Kuwertz¹⁴⁸, M. Kuze¹⁵⁸, J. Kvita¹¹⁴, A. La Rosa⁴⁹, L. La Rotonda^{37a,37b}, C. Lacasta¹⁶⁸, F. Lacava^{133a,133b}, J. Lacey²⁹, H. Lacker¹⁶, D. Lacour⁷⁹, V.R. Lacuesta¹⁶⁸, E. Ladygin⁶⁴, R. Lafaye⁵, B. Laforge⁷⁹, T. Lagouri¹⁷⁷, S. Lai⁴⁸, H. Laier^{58a}, L. Lambourne⁷⁷, S. Lammers⁶⁰, C.L. Lampen⁷, W. Lampl⁷, E. Lançon¹³⁷, U. Landgraf⁴⁸, M.P.J. Landon⁷⁵, V.S. Lang^{58a}, A.J. Lankford¹⁶⁴, F. Lanni²⁵, K. Lantzsch³⁰, S. Laplace⁷⁹, C. Lapoire²¹, J.F. Laporte¹³⁷, T. Lari^{90a}, M. Lassnig³⁰, P. Laurelli⁴⁷, W. Lavrijsen¹⁵, A.T. Law¹³⁸, P. Laycock⁷³, O. Le Dortz⁷⁹, E. Le Guirriec⁸⁴, E. Le Menedeu¹², T. LeCompte⁶, F. Ledroit-Guillon⁵⁵, C.A. Lee¹⁵², H. Lee¹⁰⁶, J.S.H. Lee¹¹⁷, S.C. Lee¹⁵², L. Lee¹⁷⁷, G. Lefebvre⁷⁹, M. Lefebvre¹⁷⁰, F. Legger⁹⁹, C. Leggett¹⁵, A. Lehan⁷³, M. Lehmacher²¹, G. Lehmann Miotto³⁰, X. Lei⁷, W.A. Leight²⁹, A. Leisos^{155,w}, A.G. Leister¹⁷⁷, M.A.L. Leite^{24d}, R. Leitner¹²⁸, D. Lellouch¹⁷³, B. Lemmer⁵⁴, K.J.C. Leney⁷⁷, T. Lenz²¹, B. Lenzi³⁰, R. Leone⁷, S. Leone^{123a,123b}, K. Leonhardt⁴⁴, C. Leonidopoulos⁴⁶, S. Leontsinis¹⁰, C. Leroy⁹⁴, C.G. Lester²⁸, C.M. Lester¹²¹, M. Levchenko¹²², J. Levêque⁵, D. Levin⁸⁸, L.J. Levinson¹⁷³, M. Levy¹⁸, A. Lewis¹¹⁹, G.H. Lewis¹⁰⁹, A.M. Leyko²¹, M. Leyton⁴¹, B. Li^{33b,x}, B. Li⁸⁴, H. Li¹⁴⁹, H.L. Li³¹, L. Li⁴⁵, L. Li^{33e}, S. Li⁴⁵, Y. Li^{33c,y}, Z. Liang¹³⁸, H. Liao³⁴, B. Liberti^{134a}, P. Lichard³⁰, K. Lie¹⁶⁶, J. Liebal²¹, W. Liebig¹⁴, C. Limbach²¹, A. Limosani⁸⁷, S.C. Lin^{152,z}, T.H. Lin⁸², F. Linde¹⁰⁶, B.E. Lindquist¹⁴⁹, J.T. Linnemann⁸⁹, E. Lipeles¹²¹, A. Lipniacka¹⁴, M. Lisovsky⁴², T.M. Liss¹⁶⁶, D. Lissauer²⁵, A. Lister¹⁶⁹, A.M. Litke¹³⁸, B. Liu^{152,aa}, D. Liu¹⁵², J.B. Liu^{33b}, K. Liu^{33b,ab}, L. Liu⁸⁸, M. Liu⁴⁵, M. Liu^{33b}, Y. Liu^{33b}, M. Livan^{120a,120b}, S.S.A. Livermore¹¹⁹, A. Lleres⁵⁵, J. Llorente Merino⁸¹, S.L. Lloyd⁷⁵, F. Lo Sterzo¹⁵², E. Lobodzinska⁴², P. Loch⁷, W.S. Lockman¹³⁸, F.K. Loebinger⁸³, A.E. Loevschall-Jensen³⁶, A. Loginov¹⁷⁷, T. Lohse¹⁶, K. Lohwasser⁴², M. Lokajicek¹²⁶, V.P. Lombardo⁵, B.A. Long²², J.D. Long⁸⁸, R.E. Long⁷¹, L. Lopes^{125a}, D. Lopez Mateos⁵⁷, B. Lopez Paredes¹⁴⁰, I. Lopez Paz¹², J. Lorenz⁹⁹, N. Lorenzo Martinez⁶⁰, M. Losada¹⁶³, P. Loscutoff¹⁵, X. Lou⁴¹, A. Lounis¹¹⁶, J. Love⁶, P.A. Love⁷¹, A.J. Lowe^{144,f}, N. Lu⁸⁸, H.J. Lubatti¹³⁹, C. Luci^{133a,133b}, A. Lucotte⁵⁵, F. Luehring⁶⁰, W. Lukas⁶¹, L. Luminari^{133a}, O. Lundberg^{147a,147b}, B. Lund-Jensen¹⁴⁸, M. Lungwitz⁸², D. Lynn²⁵, R. Lysak¹²⁶, E. Lytken⁸⁰, H. Ma²⁵, L.L. Ma^{33d}, G. Maccarrone⁴⁷, A. Macchiolo¹⁰⁰, J. Machado Miguens^{125a,125b}, D. Macina³⁰, D. Madaffari⁸⁴, R. Madar⁴⁸, H.J. Maddocks⁷¹, W.F. Mader⁴⁴, A. Madsen¹⁶⁷, T. Maeno²⁵, M. Maeno Kataoka⁸, E. Magradze⁵⁴, K. Mahboubi⁴⁸, J. Mahlstedt¹⁰⁶, S. Mahmoud⁷³, C. Maiani¹³⁷, C. Maidantchik^{24a}, A.A. Maier¹⁰⁰, A. Maio^{125a,125b,125d}, S. Majewski¹¹⁵, Y. Makida⁶⁵, N. Makovec¹¹⁶, P. Mal^{137,ac}, B. Malaescu⁷⁹, Pa. Malecki³⁹, V.P. Maleev¹²², F. Malek⁵⁵, U. Mallik⁶², D. Malon⁶, C. Malone¹⁴⁴, S. Maltezos¹⁰, V.M. Malyshev¹⁰⁸, S. Malyukov³⁰, J. Mamuzic¹³, B. Mandelli³⁰, L. Mandelli^{90a}, I. Mandić⁷⁴, R. Mandrysch⁶², J. Maneira^{125a,125b}, A. Manfredini¹⁰⁰, L. Manhaes de Andrade Filho^{24b}, J. Manjarres Ramos^{160b}, A. Mann⁹⁹, P.M. Manning¹³⁸, A. Manousakis-Katsikakis⁹, B. Mansoulie¹³⁷, R. Mantifel⁸⁶, L. Mapelli³⁰, L. March^{146c}, J.F. Marchand²⁹, G. Marchiori⁷⁹, M. Marcisovsky¹²⁶, C.P. Marino¹⁷⁰, M. Marjanovic¹³, C.N. Marques^{125a}, F. Marroquim^{24a}, S.P. Marsden⁸³, Z. Marshall¹⁵, L.F. Marti¹⁷, S. Marti-Garcia¹⁶⁸, B. Martin³⁰, B. Martin⁸⁹, T.A. Martin¹⁷¹, V.J. Martin⁴⁶, B. Martin dit Latour¹⁴, H. Martinez¹³⁷, M. Martinez^{12,p}, S. Martin-Haugh¹³⁰, A.C. Martyniuk⁷⁷, M. Marx¹³⁹, F. Marzano^{133a}, A. Marzin³⁰, L. Masetti⁸², T. Mashimo¹⁵⁶, R. Mashinistov⁹⁵, J. Masik⁸³, A.L. Maslennikov^{108,c}, I. Massa^{20a,20b}, L. Massa^{20a,20b}, N. Massol⁵, P. Mastrandrea¹⁴⁹, A. Mastroberardino^{37a,37b}, T. Masubuchi¹⁵⁶, P. Mättig¹⁷⁶, J. Mattmann⁸², J. Maurer^{26a}, S.J. Maxfield⁷³, D.A. Maximov^{108,c}, R. Mazini¹⁵², L. Mazzaferro^{134a,134b}, G. Mc Goldrick¹⁵⁹, S.P. Mc Kee⁸⁸, A. McCarn⁸⁸, R.L. McCarthy¹⁴⁹, T.G. McCarthy²⁹, N.A. McCubbin¹³⁰, K.W. McFarlane^{56,*}, J.A. Mcfayden⁷⁷, G. Mchedlidze⁵⁴, S.J. McMahon¹³⁰, R.A. McPherson^{170,l}, A. Meade⁸⁵, J. Mechnich¹⁰⁶, M. Medinnis⁴², S. Meehan³¹, S. Mehlhase⁹⁹, A. Mehta⁷³, K. Meier^{58a}, C. Meineck⁹⁹, B. Meirose⁸⁰, C. Melachrinos³¹, B.R. Mellado Garcia^{146c}, F. Meloni¹⁷, A. Mengarelli^{20a,20b}, S. Menke¹⁰⁰, E. Meoni¹⁶², K.M. Mercurio⁵⁷, S. Mergelmeyer²¹, N. Meric¹³⁷, P. Mermod⁴⁹, L. Merola^{103a,103b}, C. Meroni^{90a},

F.S. Merritt³¹, H. Merritt¹¹⁰, A. Messina^{30,ad}, J. Metcalfe²⁵, A.S. Mete¹⁶⁴, C. Meyer⁸², C. Meyer¹²¹, J.-P. Meyer¹³⁷, J. Meyer³⁰, R.P. Middleton¹³⁰, S. Migas⁷³, L. Mijović²¹, G. Mikenberg¹⁷³, M. Mikestikova¹²⁶, M. Mikuž⁷⁴, A. Milic³⁰, D.W. Miller³¹, C. Mills⁴⁶, A. Milov¹⁷³, D.A. Milstead^{147a,147b}, D. Milstein¹⁷³, A.A. Minaenko¹²⁹, I.A. Minashvili⁶⁴, A.I. Mincer¹⁰⁹, B. Mindur^{38a}, M. Mineev⁶⁴, Y. Ming¹⁷⁴, L.M. Mir¹², G. Mirabelli^{133a}, T. Mitani¹⁷², J. Mitrevski⁹⁹, V.A. Mitsou¹⁶⁸, S. Mitsui⁶⁵, A. Miucci⁴⁹, P.S. Miyagawa¹⁴⁰, J.U. Mjörnmark⁸⁰, T. Moa^{147a,147b}, K. Mochizuki⁸⁴, S. Mohapatra³⁵, W. Mohr⁴⁸, S. Molander^{147a,147b}, R. Moles-Valls¹⁶⁸, K. Mönig⁴², C. Monini⁵⁵, J. Monk³⁶, E. Monnier⁸⁴, J. Montejo Berlingen¹², F. Monticelli⁷⁰, S. Monzani^{133a,133b}, R.W. Moore³, A. Moraes⁵³, N. Morange⁶², D. Moreno⁸², M. Moreno Llácer⁵⁴, P. Morettini^{50a}, M. Morgenstern⁴⁴, M. Morii⁵⁷, S. Moritz⁸², A.K. Morley¹⁴⁸, G. Mornacchi³⁰, J.D. Morris⁷⁵, L. Morvaj¹⁰², H.G. Moser¹⁰⁰, M. Mosidze^{51b}, J. Moss¹¹⁰, K. Motohashi¹⁵⁸, R. Mount¹⁴⁴, E. Mountricha²⁵, S.V. Mouraviev^{95,*}, E.J.W. Moyse⁸⁵, S. Muanza⁸⁴, R.D. Mudd¹⁸, F. Mueller^{58a}, J. Mueller¹²⁴, K. Mueller²¹, T. Mueller²⁸, T. Mueller⁸², D. Muenstermann⁴⁹, Y. Munwes¹⁵⁴, J.A. Murillo Quijada¹⁸, W.J. Murray^{171,130}, H. Musheghyan⁵⁴, E. Musto¹⁵³, A.G. Myagkov^{129,ae}, M. Myska¹²⁷, O. Nackenhorst⁵⁴, J. Nadal⁵⁴, K. Nagai⁶¹, R. Nagai¹⁵⁸, Y. Nagai⁸⁴, K. Nagano⁶⁵, A. Nagarkar¹¹⁰, Y. Nagasaka⁵⁹, M. Nagel¹⁰⁰, A.M. Nairz³⁰, Y. Nakahama³⁰, K. Nakamura⁶⁵, T. Nakamura¹⁵⁶, I. Nakano¹¹¹, H. Namasivayam⁴¹, G. Nanava²¹, R. Narayan^{58b}, T. Nattermann²¹, T. Naumann⁴², G. Navarro¹⁶³, R. Nayyar⁷, H.A. Neal⁸⁸, P.Yu. Nechaeva⁹⁵, T.J. Neep⁸³, P.D. Nef¹⁴⁴, A. Negri^{120a,120b}, G. Negri³⁰, M. Negrini^{20a}, S. Nektarijevic⁴⁹, A. Nelson¹⁶⁴, T.K. Nelson¹⁴⁴, S. Nemecek¹²⁶, P. Nemethy¹⁰⁹, A.A. Nepomuceno^{24a}, M. Nessi^{30,af}, M.S. Neubauer¹⁶⁶, M. Neumann¹⁷⁶, R.M. Neves¹⁰⁹, P. Nevski²⁵, P.R. Newman¹⁸, D.H. Nguyen⁶, R.B. Nickerson¹¹⁹, R. Nicolaidou¹³⁷, B. Nicquevert³⁰, J. Nielsen¹³⁸, N. Nikiforou³⁵, A. Nikiforov¹⁶, V. Nikolaenko^{129,ae}, I. Nikolic-Audit⁷⁹, K. Nikolics⁴⁹, K. Nikolopoulos¹⁸, P. Nilsson⁸, Y. Ninomiya¹⁵⁶, A. Nisati^{133a}, R. Nisius¹⁰⁰, T. Nobe¹⁵⁸, L. Nodulman⁶, M. Nomachi¹¹⁷, I. Nomidis²⁹, S. Norberg¹¹², M. Nordberg³⁰, O. Novgorodova⁴⁴, S. Nowak¹⁰⁰, M. Nozaki⁶⁵, L. Nozka¹¹⁴, K. Ntekas¹⁰, G. Nunes Hanninger⁸⁷, T. Nunnemann⁹⁹, E. Nurse⁷⁷, F. Nuti⁸⁷, B.J. O'Brien⁴⁶, F. O'grady⁷, D.C. O'Neil¹⁴³, V. O'Shea⁵³, F.G. Oakham^{29,e}, H. Oberlack¹⁰⁰, T. Obermann²¹, J. Ocariz⁷⁹, A. Ochi⁶⁶, I. Ochoa⁷⁷, S. Oda⁶⁹, S. Odaka⁶⁵, H. Ogren⁶⁰, A. Oh⁸³, S.H. Oh⁴⁵, C.C. Ohm¹⁵, H. Ohman¹⁶⁷, W. Okamura¹¹⁷, H. Okawa²⁵, Y. Okumura³¹, T. Okuyama¹⁵⁶, A. Olariu^{26a}, A.G. Olchevski⁶⁴, S.A. Olivares Pino⁴⁶, D. Oliveira Damazio²⁵, E. Oliver Garcia¹⁶⁸, A. Olszewski³⁹, J. Olszowska³⁹, A. Onofre^{125a,125e}, P.U.E. Onyisi^{31,q}, C.J. Oram^{160a}, M.J. Oreglia³¹, Y. Oren¹⁵⁴, D. Orestano^{135a,135b}, N. Orlando^{72a,72b}, C. Oropeza Barrera⁵³, R.S. Orr¹⁵⁹, B. Osculati^{50a,50b}, R. Ospanov¹²¹, G. Otero y Garzon²⁷, H. Otono⁶⁹, M. Ouchrif^{136d}, E.A. Ouellette¹⁷⁰, F. Ould-Saada¹¹⁸, A. Ouraou¹³⁷, K.P. Oussoren¹⁰⁶, Q. Ouyang^{33a}, A. Ovcharova¹⁵, M. Owen⁸³, V.E. Ozcan^{19a}, N. Ozturk⁸, K. Pachal¹¹⁹, A. Pacheco Pages¹², C. Padilla Aranda¹², M. Pagáčová⁴⁸, S. Pagan Griso¹⁵, E. Paganis¹⁴⁰, C. Pahl¹⁰⁰, F. Paige²⁵, P. Pais⁸⁵, K. Pajchel¹¹⁸, G. Palacino^{160b}, S. Palestini³⁰, M. Palka^{38b}, D. Pallin³⁴, A. Palma^{125a,125b}, J.D. Palmer¹⁸, Y.B. Pan¹⁷⁴, E. Panagiotopoulou¹⁰, J.G. Panduro Vazquez⁷⁶, P. Pani¹⁰⁶, N. Panikashvili⁸⁸, S. Panitkin²⁵, D. Pantea^{26a}, L. Paolozzi^{134a,134b}, Th.D. Papadopoulos¹⁰, K. Papageorgiou¹⁵⁵, A. Paramonov⁶, D. Paredes Hernandez³⁴, M.A. Parker²⁸, F. Parodi^{50a,50b}, J.A. Parsons³⁵, U. Parzefall⁴⁸, E. Pasqualucci^{133a}, S. Passaggio^{50a}, A. Passeri^{135a}, F. Pastore^{135a,135b,*}, Fr. Pastore⁷⁶, G. Pásztor²⁹, S. Pataria¹⁷⁶, N.D. Patel¹⁵¹, J.R. Pater⁸³, S. Patricelli^{103a,103b}, T. Pauly³⁰, J. Pearce¹⁷⁰, M. Pedersen¹¹⁸, S. Pedraza Lopez¹⁶⁸, R. Pedro^{125a,125b}, S.V. Peleganchuk^{108,c}, D. Pelikan¹⁶⁷, H. Peng^{33b}, B. Penning³¹, J. Penwell⁶⁰, D.V. Perepelitsa²⁵, E. Perez Codina^{160a}, M.T. Pérez García-Estañ¹⁶⁸, V. Perez Reale³⁵, L. Perini^{90a,90b}, H. Pernegger³⁰, R. Perrino^{72a}, R. Peschke⁴², V.D. Peshekhonov⁶⁴, K. Peters³⁰, R.F.Y. Peters⁸³, B.A. Petersen³⁰, T.C. Petersen³⁶, E. Petit⁴², A. Petridis^{147a,147b}, C. Petridou¹⁵⁵, E. Petrolu^{133a}, F. Petrucci^{135a,135b}, N.E. Pettersson¹⁵⁸, R. Pezoa^{32b}, P.W. Phillips¹³⁰, G. Piacquadio¹⁴⁴, E. Pianori¹⁷¹, A. Picazio⁴⁹, E. Piccaro⁷⁵, M. Piccinini^{20a,20b}, R. Piegaia²⁷, D.T. Pignotti¹¹⁰, J.E. Pilcher³¹, A.D. Pilkington⁷⁷, J. Pina^{125a,125b,125d}, M. Pinamonti^{165a,165c,ag}, A. Pinder¹¹⁹, J.L. Pinfold³, A. Pingel³⁶, B. Pinto^{125a}, S. Pires⁷⁹, M. Pitt¹⁷³, C. Pizio^{90a,90b}, L. Plazak^{145a}, M.-A. Pleier²⁵, V. Pleskot¹²⁸, E. Plotnikova⁶⁴, P. Plucinski^{147a,147b}, S. Poddar^{58a}, F. Podlyski³⁴, R. Poettgen⁸², L. Poggioli¹¹⁶, D. Pohl²¹, M. Pohl⁴⁹, G. Polesello^{120a}, A. Policicchio^{37a,37b}, R. Polifka¹⁵⁹, A. Polini^{20a}, C.S. Pollard⁴⁵, V. Polychronakos²⁵, K. Pommès³⁰, L. Pontecorvo^{133a}, B.G. Pope⁸⁹, G.A. Popeneciu^{26b}, D.S. Popovic¹³, A. Poppleton³⁰, X. Portell Bueso¹², S. Pospisil¹²⁷, K. Potamianos¹⁵, I.N. Potrap⁶⁴, C.J. Potter¹⁵⁰,

C.T. Potter¹¹⁵, G. Poulard³⁰, J. Poveda⁶⁰, V. Pozdnyakov⁶⁴, P. Pralavorio⁸⁴, A. Pranko¹⁵, S. Prasad³⁰, R. Pravahan⁸, S. Prell⁶³, D. Price⁸³, J. Price⁷³, L.E. Price⁶, D. Prieur¹²⁴, M. Primavera^{72a}, M. Proissl⁴⁶, K. Prokofiev⁴⁷, F. Prokoshin^{32b}, E. Protopapadaki¹³⁷, S. Protopopescu²⁵, J. Proudfoot⁶, M. Przybycien^{38a}, H. Przysiezniak⁵, E. Ptacek¹¹⁵, D. Puddu^{135a,135b}, E. Pueschel⁸⁵, D. Poldon¹⁴⁹, M. Purohit^{25,ah}, P. Puzo¹¹⁶, J. Qian⁸⁸, G. Qin⁵³, Y. Qin⁸³, A. Quadt⁵⁴, D.R. Quarrie¹⁵, W.B. Quayle^{165a,165b}, M. Queitsch-Maitland⁸³, D. Quilty⁵³, A. Qureshi^{160b}, V. Radeka²⁵, V. Radescu⁴², S.K. Radhakrishnan¹⁴⁹, P. Radloff¹¹⁵, P. Rados⁸⁷, F. Ragusa^{90a,90b}, G. Rahal¹⁷⁹, S. Rajagopalan²⁵, M. Rammensee³⁰, A.S. Randle-Conde⁴⁰, C. Rangel-Smith¹⁶⁷, K. Rao¹⁶⁴, F. Rauscher⁹⁹, T.C. Rave⁴⁸, T. Ravenscroft⁵³, M. Raymond³⁰, A.L. Read¹¹⁸, N.P. Readioff⁷³, D.M. Rebuzzi^{120a,120b}, A. Redelbach¹⁷⁵, G. Redlinger²⁵, R. Reece¹³⁸, K. Reeves⁴¹, L. Rehnisch¹⁶, H. Reisin²⁷, M. Relich¹⁶⁴, C. Rembser³⁰, H. Ren^{33a}, Z.L. Ren¹⁵², A. Renaud¹¹⁶, M. Rescigno^{133a}, S. Resconi^{90a}, O.L. Rezanova^{108,c}, P. Reznicek¹²⁸, R. Rezvani⁹⁴, R. Richter¹⁰⁰, M. Ridel⁷⁹, P. Rieck¹⁶, J. Rieger⁵⁴, M. Rijssenbeek¹⁴⁹, A. Rimoldi^{120a,120b}, L. Rinaldi^{20a}, E. Ritsch⁶¹, I. Riu¹², F. Rizatdinova¹¹³, E. Rizvi⁷⁵, S.H. Robertson^{86,l}, A. Robichaud-Veronneau⁸⁶, D. Robinson²⁸, J.E.M. Robinson⁸³, A. Robson⁵³, C. Roda^{123a,123b}, L. Rodrigues³⁰, S. Roe³⁰, O. Röhne¹¹⁸, S. Rolli¹⁶², A. Romaniouk⁹⁷, M. Romano^{20a,20b}, E. Romero Adam¹⁶⁸, N. Rompotis¹³⁹, M. Ronzani⁴⁸, L. Roos⁷⁹, E. Ros¹⁶⁸, S. Rosati^{133a}, K. Rosbach⁴⁹, M. Rose⁷⁶, P. Rose¹³⁸, P.L. Rosendahl¹⁴, O. Rosenthal¹⁴², V. Rossetti^{147a,147b}, E. Rossi^{103a,103b}, L.P. Rossi^{50a}, R. Rosten¹³⁹, M. Rotaru^{26a}, I. Roth¹⁷³, J. Rothberg¹³⁹, D. Rousseau¹¹⁶, C.R. Royon¹³⁷, A. Rozanov⁸⁴, Y. Rozen¹⁵³, X. Ruan^{146c}, F. Rubbo¹², I. Rubinskiy⁴², V.I. Rud⁹⁸, C. Rudolph⁴⁴, M.S. Rudolph¹⁵⁹, F. Rühr⁴⁸, A. Ruiz-Martinez³⁰, Z. Rurikova⁴⁸, N.A. Rusakovich⁶⁴, A. Ruschke⁹⁹, J.P. Rutherford⁷, N. Ruthmann⁴⁸, Y.F. Ryabov¹²², M. Rybar¹²⁸, G. Rybkin¹¹⁶, N.C. Ryder¹¹⁹, A.F. Saavedra¹⁵¹, S. Sacerdoti²⁷, A. Saddique³, I. Sadeh¹⁵⁴, H.F-W. Sadrozinski¹³⁸, R. Sadykov⁶⁴, F. Safai Tehrani^{133a}, H. Sakamoto¹⁵⁶, Y. Sakurai¹⁷², G. Salamanna^{135a,135b}, A. Salamon^{134a}, M. Saleem¹¹², D. Salek¹⁰⁶, P.H. Sales De Bruin¹³⁹, D. Salihagic¹⁰⁰, A. Salnikov¹⁴⁴, J. Salt¹⁶⁸, D. Salvatore^{37a,37b}, F. Salvatore¹⁵⁰, A. Salvucci¹⁰⁵, A. Salzburger³⁰, D. Sampsonidis¹⁵⁵, A. Sanchez^{103a,103b}, J. Sánchez¹⁶⁸, V. Sanchez Martinez¹⁶⁸, H. Sandaker¹⁴, R.L. Sandbach⁷⁵, H.G. Sander⁸², M.P. Sanders⁹⁹, M. Sandhoff¹⁷⁶, T. Sandoval²⁸, C. Sandoval¹⁶³, R. Sandstroem¹⁰⁰, D.P.C. Sankey¹³⁰, A. Sansoni⁴⁷, C. Santoni³⁴, R. Santonico^{134a,134b}, H. Santos^{125a}, I. Santoyo Castillo¹⁵⁰, K. Sapp¹²⁴, A. Saprionov⁶⁴, J.G. Saraiva^{125a,125d}, B. Sarrazin²¹, G. Sartisohn¹⁷⁶, O. Sasaki⁶⁵, Y. Sasaki¹⁵⁶, G. Sauvage^{5,*}, E. Sauvan⁵, P. Savard^{159,e}, D.O. Savu³⁰, C. Sawyer¹¹⁹, L. Sawyer^{78,o}, D.H. Saxon⁵³, J. Saxon¹²¹, C. Sbarra^{20a}, A. Sbrizzi³, T. Scanlon⁷⁷, D.A. Scannicchio¹⁶⁴, M. Scarcella¹⁵¹, V. Scarfone^{37a,37b}, J. Schaarschmidt¹⁷³, P. Schacht¹⁰⁰, D. Schaefer³⁰, R. Schaefer⁴², S. Schaepe²¹, S. Schaetzel^{58b}, U. Schäfer⁸², A.C. Schaffer¹¹⁶, D. Schaile⁹⁹, R.D. Schamberger¹⁴⁹, V. Scharf^{58a}, V.A. Schegelsky¹²², D. Scheirich¹²⁸, M. Schernau¹⁶⁴, M.I. Scherzer³⁵, C. Schiavi^{50a,50b}, J. Schieck⁹⁹, C. Schillo⁴⁸, M. Schioppa^{37a,37b}, S. Schlenker³⁰, E. Schmidt⁴⁸, K. Schmieden³⁰, C. Schmitt⁸², S. Schmitt^{58b}, B. Schneider¹⁷, Y.J. Schnellbach⁷³, U. Schnoor⁴⁴, L. Schoeffel¹³⁷, A. Schoening^{58b}, B.D. Schoenrock⁸⁹, A.L.S. Schorlemmer⁵⁴, M. Schott⁸², D. Schouten^{160a}, J. Schovancova²⁵, S. Schramm¹⁵⁹, M. Schreyer¹⁷⁵, C. Schroeder⁸², N. Schuh⁸², M.J. Schultens²¹, H.-C. Schultz-Coulon^{58a}, H. Schulz¹⁶, M. Schumacher⁴⁸, B.A. Schumm¹³⁸, Ph. Schune¹³⁷, C. Schwanenberger⁸³, A. Schwartzman¹⁴⁴, Ph. Schwegler¹⁰⁰, Ph. Schwemling¹³⁷, R. Schwienhorst⁸⁹, J. Schwindling¹³⁷, T. Schwindt²¹, M. Schwoerer⁵, F.G. Sciacca¹⁷, E. Scifo¹¹⁶, G. Sciolla²³, W.G. Scott¹³⁰, F. Scuri^{123a,123b}, F. Scutti²¹, J. Searcy⁸⁸, G. Sedov⁴², E. Sedykh¹²², S.C. Seidel¹⁰⁴, A. Seiden¹³⁸, F. Seifert¹²⁷, J.M. Seixas^{24a}, G. Sekhniadze^{103a}, S.J. Sekula⁴⁰, K.E. Selbach⁴⁶, D.M. Seliverstov^{122,*}, G. Sellers⁷³, N. Semprini-Cesari^{20a,20b}, C. Serfon³⁰, L. Serin¹¹⁶, L. Serkin⁵⁴, T. Serre⁸⁴, R. Seuster^{160a}, H. Severini¹¹², T. Sfiligoi⁷⁴, F. Sforza¹⁰⁰, A. Sfyrly³⁰, E. Shabalina⁵⁴, M. Shamim¹¹⁵, L.Y. Shan^{33a}, R. Shang¹⁶⁶, J.T. Shank²², M. Shapiro¹⁵, P.B. Shatalov⁹⁶, K. Shaw^{165a,165b}, C.Y. Shehu¹⁵⁰, P. Sherwood⁷⁷, L. Shi^{152,ai}, S. Shimizu⁶⁶, C.O. Shimmin¹⁶⁴, M. Shimojima¹⁰¹, M. Shiyakova⁶⁴, A. Shmeleva⁹⁵, M.J. Shochet³¹, D. Short¹¹⁹, S. Shrestha⁶³, E. Shulga⁹⁷, M.A. Shupe⁷, S. Shushkevich⁴², P. Sicho¹²⁶, O. Sidiropoulou¹⁵⁵, D. Sidorov¹¹³, A. Sidoti^{133a}, F. Siegert⁴⁴, Dj. Sijacki¹³, J. Silva^{125a,125d}, Y. Silver¹⁵⁴, D. Silverstein¹⁴⁴, S.B. Silverstein^{147a}, V. Simak¹²⁷, O. Simard⁵, Lj. Simic¹³, S. Simion¹¹⁶, E. Simioni⁸², B. Simmons⁷⁷, R. Simoniello^{90a,90b}, M. Simonyan³⁶, P. Sinervo¹⁵⁹, N.B. Sinev¹¹⁵, V. Sipica¹⁴², G. Siragusa¹⁷⁵, A. Sircar⁷⁸, A.N. Sisakyan^{64,*}, S.Yu. Sivoklov⁹⁸, J. Sjölin^{147a,147b}, T.B. Sjursen¹⁴, H.P. Skottowe⁵⁷, K.Yu. Skovpen¹⁰⁸, P. Skubic¹¹², M. Slater¹⁸, T. Slavicek¹²⁷, K. Sliwa¹⁶², V. Smakhtin¹⁷³,

B.H. Smart⁴⁶, L. Smestad¹⁴, S.Yu. Smirnov⁹⁷, Y. Smirnov⁹⁷, L.N. Smirnova^{98,aj}, O. Smirnova⁸⁰, K.M. Smith⁵³, M. Smizanska⁷¹, K. Smolek¹²⁷, A.A. Snesev⁹⁵, G. Snidero⁷⁵, S. Snyder²⁵, R. Sobie^{170,l}, F. Socher⁴⁴, A. Soffer¹⁵⁴, D.A. Soh^{152,ai}, C.A. Solans³⁰, M. Solar¹²⁷, J. Solc¹²⁷, E.Yu. Soldatov⁹⁷, U. Soldevila¹⁶⁸, A.A. Solodkov¹²⁹, A. Soloshenko⁶⁴, O.V. Solovyanov¹²⁹, V. Solovyev¹²², P. Sommer⁴⁸, H.Y. Song^{33b}, N. Soni¹, A. Sood¹⁵, A. Sopczak¹²⁷, B. Sopko¹²⁷, V. Sopko¹²⁷, V. Sorin¹², M. Sosebee⁸, R. Soualah^{165a,165c}, P. Soueid⁹⁴, A.M. Soukharev^{108,c}, D. South⁴², S. Spagnolo^{72a,72b}, F. Spanò⁷⁶, W.R. Spearman⁵⁷, F. Spettel¹⁰⁰, R. Spighi^{20a}, G. Spigo³⁰, L.A. Spiller⁸⁷, M. Spousta¹²⁸, T. Spreitzer¹⁵⁹, B. Spurlock⁸, R.D. St. Denis^{53,*}, S. Staerz⁴⁴, J. Stahlman¹²¹, R. Stamen^{58a}, S. Stamm¹⁶, E. Stanecka³⁹, R.W. Stanek⁶, C. Stanescu^{135a}, M. Stanescu-Bellu⁴², M.M. Stanitzki⁴², S. Stapnes¹¹⁸, E.A. Starchenko¹²⁹, J. Stark⁵⁵, P. Staroba¹²⁶, P. Starovoitov⁴², R. Staszewski³⁹, P. Stavina^{145a,*}, P. Steinberg²⁵, B. Stelzer¹⁴³, H.J. Stelzer³⁰, O. Stelzer-Chilton^{160a}, H. Stenzel⁵², S. Stern¹⁰⁰, G.A. Stewart⁵³, J.A. Stillings²¹, M.C. Stockton⁸⁶, M. Stoebe⁸⁶, G. Stoica^{26a}, P. Stolte⁵⁴, S. Stonjek¹⁰⁰, A.R. Stradling⁸, A. Straessner⁴⁴, M.E. Stramaglia¹⁷, J. Strandberg¹⁴⁸, S. Strandberg^{147a,147b}, A. Strandlie¹¹⁸, E. Strauss¹⁴⁴, M. Strauss¹¹², P. Strizenec^{145b}, R. Ströhmer¹⁷⁵, D.M. Strom¹¹⁵, R. Stroynowski⁴⁰, S.A. Stucci¹⁷, B. Stugu¹⁴, N.A. Styles⁴², D. Su¹⁴⁴, J. Su¹²⁴, R. Subramaniam⁷⁸, A. Succurro¹², Y. Sugaya¹¹⁷, C. Suhr¹⁰⁷, M. Suk¹²⁷, V.V. Sulin⁹⁵, S. Sultansoy^{4c}, T. Sumida⁶⁷, S. Sun⁵⁷, X. Sun^{33a}, J.E. Sundermann⁴⁸, K. Suruliz¹⁴⁰, G. Susinno^{37a,37b}, M.R. Sutton¹⁵⁰, Y. Suzuki⁶⁵, M. Svatos¹²⁶, S. Swedish¹⁶⁹, M. Swiatkowski¹⁴⁴, I. Sykora^{145a}, T. Sykora¹²⁸, D. Ta⁸⁹, C. Taccini^{135a,135b}, K. Tackmann⁴², J. Taenzer¹⁵⁹, A. Taffard¹⁶⁴, R. Tahirout^{160a}, N. Taiblum¹⁵⁴, H. Takai²⁵, R. Takashima⁶⁸, H. Takeda⁶⁶, T. Takeshita¹⁴¹, Y. Takubo⁶⁵, M. Talby⁸⁴, A.A. Talyshev^{108,c}, J.Y.C. Tam¹⁷⁵, K.G. Tan⁸⁷, J. Tanaka¹⁵⁶, R. Tanaka¹¹⁶, S. Tanaka¹³², S. Tanaka⁶⁵, A.J. Tanasijczuk¹⁴³, B.B. Tannenwald¹¹⁰, N. Tannoury²¹, S. Tapprogge⁸², S. Tarem¹⁵³, F. Tarrade²⁹, G.F. Tartarelli^{90a}, P. Tas¹²⁸, M. Tasevsky¹²⁶, T. Tashiro⁶⁷, E. Tassi^{37a,37b}, A. Tavares Delgado^{125a,125b}, Y. Tayalati^{136d}, F.E. Taylor⁹³, G.N. Taylor⁸⁷, W. Taylor^{160b}, F.A. Teischinger³⁰, M. Teixeira Dias Castanheira⁷⁵, P. Teixeira-Dias⁷⁶, K.K. Temming⁴⁸, H. Ten Kate³⁰, P.K. Teng¹⁵², J.J. Teoh¹¹⁷, S. Terada⁶⁵, K. Terashi¹⁵⁶, J. Terron⁸¹, S. Terzo¹⁰⁰, M. Testa⁴⁷, R.J. Teuscher^{159,l}, J. Therhaag²¹, T. Theveneaux-Pelzer³⁴, J.P. Thomas¹⁸, J. Thomas-Wilsker⁷⁶, E.N. Thompson³⁵, P.D. Thompson¹⁸, P.D. Thompson¹⁵⁹, R.J. Thompson⁸³, A.S. Thompson⁵³, L.A. Thomsen³⁶, E. Thomson¹²¹, M. Thomson²⁸, W.M. Thong⁸⁷, R.P. Thun^{88,*}, F. Tian³⁵, M.J. Tibbetts¹⁵, V.O. Tikhomirov^{95,ak}, Yu.A. Tikhonov^{108,c}, S. Timoshenko⁹⁷, E. Tiouchichine⁸⁴, P. Tipton¹⁷⁷, S. Tisserant⁸⁴, T. Todorov^{5,*}, S. Todorova-Nova¹²⁸, B. Toggerson⁷, J. Tojo⁶⁹, S. Tokár^{145a}, K. Tokushuku⁶⁵, K. Tollefson⁸⁹, L. Tomlinson⁸³, M. Tomoto¹⁰², L. Tompkins³¹, K. Toms¹⁰⁴, N.D. Topilin⁶⁴, E. Torrence¹¹⁵, H. Torres¹⁴³, E. Torró Pastor¹⁶⁸, J. Toth^{84,al}, F. Touchard⁸⁴, D.R. Tovey¹⁴⁰, H.L. Tran¹¹⁶, T. Trefzger¹⁷⁵, L. Tremblet³⁰, A. Tricoli³⁰, I.M. Trigger^{160a}, S. Trincaz-Duvoid⁷⁹, M.F. Tripiana¹², W. Trischuk¹⁵⁹, B. Trocmé⁵⁵, C. Troncon^{90a}, M. Trottier-McDonald¹⁴³, M. Trovatelli^{135a,135b}, P. True⁸⁹, M. Trzebinski³⁹, A. Trzupek³⁹, C. Tsarouchas³⁰, J.C.-L. Tseng¹¹⁹, P.V. Tsiarehka⁹¹, D. Tsionou¹³⁷, G. Tsipolitis¹⁰, N. Tsirintanis⁹, S. Tsiskaridze¹², V. Tsiskaridze⁴⁸, E.G. Tskhadadze^{51a}, I.I. Tsukerman⁹⁶, V. Tsulaia¹⁵, S. Tsuno⁶⁵, D. Tsybychev¹⁴⁹, A. Tudorache^{26a}, V. Tudorache^{26a}, A.N. Tuna¹²¹, S.A. Tupputi^{20a,20b}, S. Turchikho^{98,aj}, D. Turecek¹²⁷, R. Turra^{90a,90b}, P.M. Tuts³⁵, A. Tykhonov⁴⁹, M. Tylmad^{147a,147b}, M. Tyndel¹³⁰, K. Uchida²¹, I. Ueda¹⁵⁶, R. Ueno²⁹, M. Ughetto⁸⁴, M. Ugland¹⁴, M. Uhlenbrock²¹, F. Ukegawa¹⁶¹, G. Unal³⁰, A. Undrus²⁵, G. Unel¹⁶⁴, F.C. Ungaro⁴⁸, Y. Unno⁶⁵, C. Unverdorben⁹⁹, D. Urbaniec³⁵, P. Urquijo⁸⁷, G. Usai⁸, A. Usanova⁶¹, L. Vacavant⁸⁴, V. Vacek¹²⁷, B. Vachon⁸⁶, N. Valencic¹⁰⁶, S. Valentinetti^{20a,20b}, A. Valero¹⁶⁸, L. Valery³⁴, S. Valkar¹²⁸, E. Valladolid Gallego¹⁶⁸, S. Vallecorsa⁴⁹, J.A. Valls Ferrer¹⁶⁸, W. Van Den Wollenberg¹⁰⁶, P.C. Van Der Deijl¹⁰⁶, R. van der Geer¹⁰⁶, H. van der Graaf¹⁰⁶, R. Van Der Leeuw¹⁰⁶, D. van der Ster³⁰, N. van Eldik³⁰, P. van Gemmeren⁶, J. Van Nieuwkoop¹⁴³, I. van Vulpen¹⁰⁶, M.C. van Woerden³⁰, M. Vanadia^{133a,133b}, W. Vandelli³⁰, R. Vanguri¹²¹, A. Vaniachine⁶, F. Vannucci⁷⁹, G. Vardanyan¹⁷⁸, R. Vari^{133a}, E.W. Varnes⁷, T. Varol⁸⁵, D. Varouchas⁷⁹, A. Vartapetian⁸, K.E. Varvell¹⁵¹, F. Vazeille³⁴, T. Vazquez Schroeder⁵⁴, J. Veatch⁷, F. Veloso^{125a,125c}, T. Velz²¹, S. Veneziano^{133a}, A. Ventura^{72a,72b}, D. Ventura⁸⁵, M. Venturi¹⁷⁰, N. Venturi¹⁵⁹, A. Venturini²³, V. Vercesi^{120a}, M. Verducci^{133a,133b}, W. Verkerke¹⁰⁶, J.C. Vermeulen¹⁰⁶, A. Vest⁴⁴, M.C. Vetterli^{143,e}, O. Viazlo⁸⁰, I. Vichou¹⁶⁶, T. Vickey^{146c,am}, O.E. Vickey Boeriu^{146c}, G.H.A. Viehhauser¹¹⁹, S. Viel¹⁶⁹, R. Vigne³⁰, M. Villa^{20a,20b}, M. Villaplana Perez^{90a,90b}, E. Vilucchi⁴⁷, M.G. Vincter²⁹, V.B. Vinogradov⁶⁴, J. Virzi¹⁵, I. Vivarelli¹⁵⁰,

F. Vives Vaque³, S. Vlachos¹⁰, D. Vladoiu⁹⁹, M. Vlasak¹²⁷, A. Vogel²¹, M. Vogel^{32a}, P. Vokac¹²⁷, G. Volpi^{123a,123b}, M. Volpi⁸⁷, H. von der Schmitt¹⁰⁰, H. von Radziewski⁴⁸, E. von Toerne²¹, V. Vorobel¹²⁸, K. Vorobev⁹⁷, M. Vos¹⁶⁸, R. Voss³⁰, J.H. Vosseveld⁷³, N. Vranjes¹³⁷, M. Vranjes Milosavljevic¹⁰⁶, V. Vrba¹²⁶, M. Vreeswijk¹⁰⁶, T. Vu Anh⁴⁸, R. Vuillermet³⁰, I. Vukotic³¹, Z. Vykydal¹²⁷, P. Wagner²¹, W. Wagner¹⁷⁶, H. Wahlberg⁷⁰, S. Wahrmund⁴⁴, J. Wakabayashi¹⁰², J. Walder⁷¹, R. Walker⁹⁹, W. Walkowiak¹⁴², R. Wall¹⁷⁷, P. Waller⁷³, B. Walsh¹⁷⁷, C. Wang^{152,an}, C. Wang⁴⁵, F. Wang¹⁷⁴, H. Wang¹⁵, H. Wang⁴⁰, J. Wang⁴², J. Wang^{33a}, K. Wang⁸⁶, R. Wang¹⁰⁴, S.M. Wang¹⁵², T. Wang²¹, X. Wang¹⁷⁷, C. Wanotayaroj¹¹⁵, A. Warburton⁸⁶, C.P. Ward²⁸, D.R. Wardrope⁷⁷, M. Warsinsky⁴⁸, A. Washbrook⁴⁶, C. Wasicki⁴², P.M. Watkins¹⁸, A.T. Watson¹⁸, I.J. Watson¹⁵¹, M.F. Watson¹⁸, G. Watts¹³⁹, S. Watts⁸³, B.M. Waugh⁷⁷, S. Webb⁸³, M.S. Weber¹⁷, S.W. Weber¹⁷⁵, J.S. Webster³¹, A.R. Weidberg¹¹⁹, P. Weigell¹⁰⁰, B. Weinert⁶⁰, J. Weingarten⁵⁴, C. Weiser⁴⁸, H. Weits¹⁰⁶, P.S. Wells³⁰, T. Wenaus²⁵, D. Wendland¹⁶, Z. Weng^{152,ai}, T. Wengler³⁰, S. Wenig³⁰, N. Wermes²¹, M. Werner⁴⁸, P. Werner³⁰, M. Wessels^{58a}, J. Wetter¹⁶², K. Whalen²⁹, A. White⁸, M.J. White¹, R. White^{32b}, S. White^{123a,123b}, D. Whiteson¹⁶⁴, D. Wicke¹⁷⁶, F.J. Wickens¹³⁰, W. Wiedenmann¹⁷⁴, M. Wieler¹³⁰, P. Wienemann²¹, C. Wiglesworth³⁶, L.A.M. Wiik-Fuchs²¹, P.A. Wijeratne⁷⁷, A. Wildauer¹⁰⁰, M.A. Wildt^{42,ao}, H.G. Wilkens³⁰, J.Z. Will⁹⁹, H.H. Williams¹²¹, S. Williams²⁸, C. Willis⁸⁹, S. Willocq⁸⁵, A. Wilson⁸⁸, J.A. Wilson¹⁸, I. Wingerter-Seez⁵, F. Winklmeier¹¹⁵, B.T. Winter²¹, M. Wittgen¹⁴⁴, T. Wittig⁴³, J. Wittkowski⁹⁹, S.J. Wollstadt⁸², M.W. Wolter³⁹, H. Wolters^{125a,125c}, B.K. Wosiek³⁹, J. Wotschack³⁰, M.J. Woudstra⁸³, K.W. Wozniak³⁹, M. Wright⁵³, M. Wu⁵⁵, S.L. Wu¹⁷⁴, X. Wu⁴⁹, Y. Wu⁸⁸, E. Wulf³⁵, T.R. Wyatt⁸³, B.M. Wynne⁴⁶, S. Xella³⁶, M. Xiao¹³⁷, D. Xu^{33a}, L. Xu^{33b,ap}, B. Yabsley¹⁵¹, S. Yacoub^{146b,aq}, R. Yakabe⁶⁶, M. Yamada⁶⁵, H. Yamaguchi¹⁵⁶, Y. Yamaguchi¹¹⁷, A. Yamamoto⁶⁵, K. Yamamoto⁶³, S. Yamamoto¹⁵⁶, T. Yamamura¹⁵⁶, T. Yamanaka¹⁵⁶, K. Yamauchi¹⁰², Y. Yamazaki⁶⁶, Z. Yan²², H. Yang^{33e}, H. Yang¹⁷⁴, U.K. Yang⁸³, Y. Yang¹¹⁰, S. Yanush⁹², L. Yao^{33a}, W.-M. Yao¹⁵, Y. Yasu⁶⁵, E. Yatsenko⁴², K.H. Yau Wong²¹, J. Ye⁴⁰, S. Ye²⁵, I. Yeletsikh⁶⁴, A.L. Yen⁵⁷, E. Yildirim⁴², M. Yilmaz^{4b}, R. Yoosoofmiya¹²⁴, K. Yorita¹⁷², R. Yoshida⁶, K. Yoshihara¹⁵⁶, C. Young¹⁴⁴, C.J.S. Young³⁰, S. Youssef²², D.R. Yu¹⁵, J. Yu⁸, J.M. Yu⁸⁸, J. Yu¹¹³, L. Yuan⁶⁶, A. Yurkewicz¹⁰⁷, I. Yusuf^{28,ar}, B. Zabinski³⁹, R. Zaidan⁶², A.M. Zaitsev^{129,ae}, A. Zaman¹⁴⁹, S. Zambito²³, L. Zanello^{133a,133b}, D. Zanzi¹⁰⁰, C. Zeitnitz¹⁷⁶, M. Zeman¹²⁷, A. Zemla^{38a}, K. Zengel²³, O. Zenin¹²⁹, T. Ženiš^{145a}, D. Zerwas¹¹⁶, G. Zevi della Porta⁵⁷, D. Zhang⁸⁸, F. Zhang¹⁷⁴, H. Zhang⁸⁹, J. Zhang⁶, L. Zhang¹⁵², X. Zhang^{33d}, Z. Zhang¹¹⁶, Z. Zhao^{33b}, A. Zhemchugov⁶⁴, J. Zhong¹¹⁹, B. Zhou⁸⁸, L. Zhou³⁵, N. Zhou¹⁶⁴, C.G. Zhu^{33d}, H. Zhu^{33a}, J. Zhu⁸⁸, Y. Zhu^{33b}, X. Zhuang^{33a}, K. Zhukov⁹⁵, A. Zibell¹⁷⁵, D. Zieminska⁶⁰, N.I. Zimine⁶⁴, C. Zimmermann⁸², R. Zimmermann²¹, S. Zimmermann²¹, S. Zimmermann⁴⁸, Z. Zinonos⁵⁴, M. Ziolkowski¹⁴², G. Zoernig¹⁷⁴, A. Zoccoli^{20a,20b}, M. zur Nedden¹⁶, G. Zurzolo^{103a,103b}, V. Zutshi¹⁰⁷, L. Zwalinski³⁰

¹ Department of Physics, University of Adelaide, Adelaide, Australia

² Physics Department, SUNY Albany, Albany, NY, United States

³ Department of Physics, University of Alberta, Edmonton, AB, Canada

⁴ (a) Department of Physics, Ankara University, Ankara; (b) Department of Physics, Gazi University, Ankara; (c) Division of Physics, TOBB University of Economics and Technology, Ankara;

(d) Turkish Atomic Energy Authority, Ankara, Turkey

⁵ LAPP, CNRS/IN2P3 and Université Savoie Mont Blanc, Annecy-le-Vieux, France

⁶ High Energy Physics Division, Argonne National Laboratory, Argonne, IL, United States

⁷ Department of Physics, University of Arizona, Tucson, AZ, United States

⁸ Department of Physics, The University of Texas at Arlington, Arlington, TX, United States

⁹ Physics Department, University of Athens, Athens, Greece

¹⁰ Physics Department, National Technical University of Athens, Zografou, Greece

¹¹ Institute of Physics, Azerbaijan Academy of Sciences, Baku, Azerbaijan

¹² Institut de Física d'Altes Energies and Departament de Física de la Universitat Autònoma de Barcelona, Barcelona, Spain

¹³ Institute of Physics, University of Belgrade, Belgrade, Serbia

¹⁴ Department for Physics and Technology, University of Bergen, Bergen, Norway

¹⁵ Physics Division, Lawrence Berkeley National Laboratory and University of California, Berkeley, CA, United States

¹⁶ Department of Physics, Humboldt University, Berlin, Germany

¹⁷ Albert Einstein Center for Fundamental Physics and Laboratory for High Energy Physics, University of Bern, Bern, Switzerland

¹⁸ School of Physics and Astronomy, University of Birmingham, Birmingham, United Kingdom

¹⁹ (a) Department of Physics, Bogazici University, Istanbul; (b) Department of Physics, Dogus University, Istanbul; (c) Department of Physics Engineering, Gaziantep University, Gaziantep, Turkey

²⁰ (a) INFN Sezione di Bologna; (b) Dipartimento di Fisica e Astronomia, Università di Bologna, Bologna, Italy

²¹ Physikalisches Institut, University of Bonn, Bonn, Germany

²² Department of Physics, Boston University, Boston, MA, United States

²³ Department of Physics, Brandeis University, Waltham, MA, United States

²⁴ (a) Universidade Federal do Rio De Janeiro COPPE/EE/IF, Rio de Janeiro; (b) Electrical Circuits Department, Federal University of Juiz de Fora (UFJF), Juiz de Fora; (c) Federal University of Sao Joao del Rei (UFSJ), Sao Joao del Rei; (d) Instituto de Física, Universidade de Sao Paulo, Sao Paulo, Brazil

- ²⁵ Physics Department, Brookhaven National Laboratory, Upton, NY, United States
- ²⁶ ^(a) National Institute of Physics and Nuclear Engineering, Bucharest; ^(b) National Institute for Research and Development of Isotopic and Molecular Technologies, Physics Department, Cluj Napoca; ^(c) University Politehnica Bucharest, Bucharest; ^(d) West University in Timisoara, Timisoara, Romania
- ²⁷ Departamento de Física, Universidad de Buenos Aires, Buenos Aires, Argentina
- ²⁸ Cavendish Laboratory, University of Cambridge, Cambridge, United Kingdom
- ²⁹ Department of Physics, Carleton University, Ottawa, ON, Canada
- ³⁰ CERN, Geneva, Switzerland
- ³¹ Enrico Fermi Institute, University of Chicago, Chicago, IL, United States
- ³² ^(a) Departamento de Física, Pontificia Universidad Católica de Chile, Santiago; ^(b) Departamento de Física, Universidad Técnica Federico Santa María, Valparaíso, Chile
- ³³ ^(a) Institute of High Energy Physics, Chinese Academy of Sciences, Beijing; ^(b) Department of Modern Physics, University of Science and Technology of China, Anhui; ^(c) Department of Physics, Nanjing University, Jiangsu; ^(d) School of Physics, Shandong University, Shandong; ^(e) Department of Physics and Astronomy, Shanghai Key Laboratory for Particle Physics and Cosmology, Shanghai Jiao Tong University, Shanghai, China
- ³⁴ Laboratoire de Physique Corpusculaire, Clermont Université and Université Blaise Pascal and CNRS/IN2P3, Clermont-Ferrand, France
- ³⁵ Nevis Laboratory, Columbia University, Irvington, NY, United States
- ³⁶ Niels Bohr Institute, University of Copenhagen, Copenhagen, Denmark
- ³⁷ ^(a) INFN Gruppo Collegato di Cosenza, Laboratori Nazionali di Frascati; ^(b) Dipartimento di Fisica, Università della Calabria, Rende, Italy
- ³⁸ ^(a) AGH University of Science and Technology, Faculty of Physics and Applied Computer Science, Krakow; ^(b) Marian Smoluchowski Institute of Physics, Jagiellonian University, Krakow, Poland
- ³⁹ Institute of Nuclear Physics Polish Academy of Sciences, Krakow, Poland
- ⁴⁰ Physics Department, Southern Methodist University, Dallas, TX, United States
- ⁴¹ Physics Department, University of Texas at Dallas, Richardson, TX, United States
- ⁴² DESY, Hamburg and Zeuthen, Germany
- ⁴³ Institut für Experimentelle Physik IV, Technische Universität Dortmund, Dortmund, Germany
- ⁴⁴ Institut für Kern- und Teilchenphysik, Technische Universität Dresden, Dresden, Germany
- ⁴⁵ Department of Physics, Duke University, Durham, NC, United States
- ⁴⁶ SUPA – School of Physics and Astronomy, University of Edinburgh, Edinburgh, United Kingdom
- ⁴⁷ INFN Laboratori Nazionali di Frascati, Frascati, Italy
- ⁴⁸ Fakultät für Mathematik und Physik, Albert-Ludwigs-Universität, Freiburg, Germany
- ⁴⁹ Section de Physique, Université de Genève, Geneva, Switzerland
- ⁵⁰ ^(a) INFN Sezione di Genova; ^(b) Dipartimento di Fisica, Università di Genova, Genova, Italy
- ⁵¹ ^(a) E. Andronikashvili Institute of Physics, Iv. Javakishvili Tbilisi State University, Tbilisi; ^(b) High Energy Physics Institute, Tbilisi State University, Tbilisi, Georgia
- ⁵² II Physikalisches Institut, Justus-Liebig-Universität Giessen, Giessen, Germany
- ⁵³ SUPA – School of Physics and Astronomy, University of Glasgow, Glasgow, United Kingdom
- ⁵⁴ II Physikalisches Institut, Georg-August-Universität, Göttingen, Germany
- ⁵⁵ Laboratoire de Physique Subatomique et de Cosmologie, Université Grenoble-Alpes, CNRS/IN2P3, Grenoble, France
- ⁵⁶ Department of Physics, Hampton University, Hampton, VA, United States
- ⁵⁷ Laboratory for Particle Physics and Cosmology, Harvard University, Cambridge, MA, United States
- ⁵⁸ ^(a) Kirchhoff-Institut für Physik, Ruprecht-Karls-Universität Heidelberg, Heidelberg; ^(b) Physikalisches Institut, Ruprecht-Karls-Universität Heidelberg, Heidelberg; ^(c) ZITI Institut für technische Informatik, Ruprecht-Karls-Universität Heidelberg, Mannheim, Germany
- ⁵⁹ Faculty of Applied Information Science, Hiroshima Institute of Technology, Hiroshima, Japan
- ⁶⁰ Department of Physics, Indiana University, Bloomington, IN, United States
- ⁶¹ Institut für Astro- und Teilchenphysik, Leopold-Franzens-Universität, Innsbruck, Austria
- ⁶² University of Iowa, Iowa City, IA, United States
- ⁶³ Department of Physics and Astronomy, Iowa State University, Ames, IA, United States
- ⁶⁴ Joint Institute for Nuclear Research, JINR Dubna, Dubna, Russia
- ⁶⁵ KEK, High Energy Accelerator Research Organization, Tsukuba, Japan
- ⁶⁶ Graduate School of Science, Kobe University, Kobe, Japan
- ⁶⁷ Faculty of Science, Kyoto University, Kyoto, Japan
- ⁶⁸ Kyoto University of Education, Kyoto, Japan
- ⁶⁹ Department of Physics, Kyushu University, Fukuoka, Japan
- ⁷⁰ Instituto de Física La Plata, Universidad Nacional de La Plata and CONICET, La Plata, Argentina
- ⁷¹ Physics Department, Lancaster University, Lancaster, United Kingdom
- ⁷² ^(a) INFN Sezione di Lecce; ^(b) Dipartimento di Matematica e Fisica, Università del Salento, Lecce, Italy
- ⁷³ Oliver Lodge Laboratory, University of Liverpool, Liverpool, United Kingdom
- ⁷⁴ Department of Physics, Jožef Stefan Institute and University of Ljubljana, Ljubljana, Slovenia
- ⁷⁵ School of Physics and Astronomy, Queen Mary University of London, London, United Kingdom
- ⁷⁶ Department of Physics, Royal Holloway University of London, Surrey, United Kingdom
- ⁷⁷ Department of Physics and Astronomy, University College London, London, United Kingdom
- ⁷⁸ Louisiana Tech University, Ruston, LA, United States
- ⁷⁹ Laboratoire de Physique Nucléaire et de Hautes Energies, UPMC and Université Paris-Diderot and CNRS/IN2P3, Paris, France
- ⁸⁰ Fysiska institutionen, Lunds universitet, Lund, Sweden
- ⁸¹ Departamento de Física Teórica C-15, Universidad Autónoma de Madrid, Madrid, Spain
- ⁸² Institut für Physik, Universität Mainz, Mainz, Germany
- ⁸³ School of Physics and Astronomy, University of Manchester, Manchester, United Kingdom
- ⁸⁴ CPPM, Aix-Marseille Université and CNRS/IN2P3, Marseille, France
- ⁸⁵ Department of Physics, University of Massachusetts, Amherst, MA, United States
- ⁸⁶ Department of Physics, McGill University, Montreal, QC, Canada
- ⁸⁷ School of Physics, University of Melbourne, Victoria, Australia
- ⁸⁸ Department of Physics, The University of Michigan, Ann Arbor, MI, United States
- ⁸⁹ Department of Physics and Astronomy, Michigan State University, East Lansing, MI, United States
- ⁹⁰ ^(a) INFN Sezione di Milano; ^(b) Dipartimento di Fisica, Università di Milano, Milano, Italy
- ⁹¹ B.I. Stepanov Institute of Physics, National Academy of Sciences of Belarus, Minsk, Belarus
- ⁹² National Scientific and Educational Centre for Particle and High Energy Physics, Minsk, Belarus
- ⁹³ Department of Physics, Massachusetts Institute of Technology, Cambridge, MA, United States
- ⁹⁴ Group of Particle Physics, University of Montreal, Montreal, QC, Canada
- ⁹⁵ P.N. Lebedev Institute of Physics, Academy of Sciences, Moscow, Russia
- ⁹⁶ Institute for Theoretical and Experimental Physics (ITEP), Moscow, Russia
- ⁹⁷ National Research Nuclear University MEPhI, Moscow, Russia
- ⁹⁸ D.V. Skobel'syn Institute of Nuclear Physics, M.V. Lomonosov Moscow State University, Moscow, Russia

- ⁹⁹ Fakultät für Physik, Ludwig-Maximilians-Universität München, München, Germany
- ¹⁰⁰ Max-Planck-Institut für Physik (Werner-Heisenberg-Institut), München, Germany
- ¹⁰¹ Nagasaki Institute of Applied Science, Nagasaki, Japan
- ¹⁰² Graduate School of Science and Kobayashi-Maskawa Institute, Nagoya University, Nagoya, Japan
- ¹⁰³ ^(a) INFN Sezione di Napoli; ^(b) Dipartimento di Fisica, Università di Napoli, Napoli, Italy
- ¹⁰⁴ Department of Physics and Astronomy, University of New Mexico, Albuquerque, NM, United States
- ¹⁰⁵ Institute for Mathematics, Astrophysics and Particle Physics, Radboud University Nijmegen/Nikhef, Nijmegen, Netherlands
- ¹⁰⁶ Nikhef National Institute for Subatomic Physics and University of Amsterdam, Amsterdam, Netherlands
- ¹⁰⁷ Department of Physics, Northern Illinois University, DeKalb, IL, United States
- ¹⁰⁸ Budker Institute of Nuclear Physics, SB RAS, Novosibirsk, Russia
- ¹⁰⁹ Department of Physics, New York University, New York, NY, United States
- ¹¹⁰ Ohio State University, Columbus, OH, United States
- ¹¹¹ Faculty of Science, Okayama University, Okayama, Japan
- ¹¹² Homer L. Dodge Department of Physics and Astronomy, University of Oklahoma, Norman, OK, United States
- ¹¹³ Department of Physics, Oklahoma State University, Stillwater, OK, United States
- ¹¹⁴ Palacký University, RCPTM, Olomouc, Czech Republic
- ¹¹⁵ Center for High Energy Physics, University of Oregon, Eugene, OR, United States
- ¹¹⁶ LAL, Université Paris-Sud and CNRS/IN2P3, Orsay, France
- ¹¹⁷ Graduate School of Science, Osaka University, Osaka, Japan
- ¹¹⁸ Department of Physics, University of Oslo, Oslo, Norway
- ¹¹⁹ Department of Physics, Oxford University, Oxford, United Kingdom
- ¹²⁰ ^(a) INFN Sezione di Pavia; ^(b) Dipartimento di Fisica, Università di Pavia, Pavia, Italy
- ¹²¹ Department of Physics, University of Pennsylvania, Philadelphia, PA, United States
- ¹²² National Research Centre “Kurchatov Institute”, B.P. Konstantinov Petersburg Nuclear Physics Institute, St. Petersburg, Russia
- ¹²³ ^(a) INFN Sezione di Pisa; ^(b) Dipartimento di Fisica E. Fermi, Università di Pisa, Pisa, Italy
- ¹²⁴ Department of Physics and Astronomy, University of Pittsburgh, Pittsburgh, PA, United States
- ¹²⁵ ^(a) Laboratório de Instrumentação e Física Experimental de Partículas – LIP, Lisboa; ^(b) Faculdade de Ciências, Universidade de Lisboa, Lisboa; ^(c) Department of Physics, University of Coimbra, Coimbra; ^(d) Centro de Física Nuclear da Universidade de Lisboa, Lisboa; ^(e) Departamento de Física, Universidade do Minho, Braga; ^(f) Departamento de Física Teórica y del Cosmos and CAFPE, Universidad de Granada, Granada (Spain); ^(g) Dep Física and CEFITEC of Faculdade de Ciências e Tecnologia, Universidade Nova de Lisboa, Caparica, Portugal
- ¹²⁶ Institute of Physics, Academy of Sciences of the Czech Republic, Praha, Czech Republic
- ¹²⁷ Czech Technical University in Prague, Praha, Czech Republic
- ¹²⁸ Faculty of Mathematics and Physics, Charles University in Prague, Praha, Czech Republic
- ¹²⁹ State Research Center Institute for High Energy Physics, Protvino, Russia
- ¹³⁰ Particle Physics Department, Rutherford Appleton Laboratory, Didcot, United Kingdom
- ¹³¹ Physics Department, University of Regina, Regina, SK, Canada
- ¹³² Ritsumeikan University, Kusatsu, Shiga, Japan
- ¹³³ ^(a) INFN Sezione di Roma; ^(b) Dipartimento di Fisica, Sapienza Università di Roma, Roma, Italy
- ¹³⁴ ^(a) INFN Sezione di Roma Tor Vergata; ^(b) Dipartimento di Fisica, Università di Roma Tor Vergata, Roma, Italy
- ¹³⁵ ^(a) INFN Sezione di Roma Tre; ^(b) Dipartimento di Matematica e Fisica, Università Roma Tre, Roma, Italy
- ¹³⁶ ^(a) Faculté des Sciences Ain Chock, Réseau Universitaire de Physique des Hautes Energies – Université Hassan II, Casablanca; ^(b) Centre National de l'Energie des Sciences Techniques Nucleaires, Rabat; ^(c) Faculté des Sciences Semlalia, Université Cadi Ayyad, LPHEA-Marrakech; ^(d) Faculté des Sciences, Université Mohamed Premier and LPTPM, Oujda;
- ¹³⁷ Faculté des sciences, Université Mohammed V-Agdal, Rabat, Morocco
- ¹³⁸ DSM/IRFU (Institut de Recherches sur les Lois Fondamentales de l'Univers), CEA Saclay (Commissariat à l'Energie Atomique et aux Energies Alternatives), Gif-sur-Yvette, France
- ¹³⁹ Santa Cruz Institute for Particle Physics, University of California Santa Cruz, Santa Cruz, CA, United States
- ¹⁴⁰ Department of Physics, University of Washington, Seattle, WA, United States
- ¹⁴¹ Department of Physics and Astronomy, University of Sheffield, Sheffield, United Kingdom
- ¹⁴² Department of Physics, Shinshu University, Nagano, Japan
- ¹⁴³ Fachbereich Physik, Universität Siegen, Siegen, Germany
- ¹⁴⁴ Department of Physics, Simon Fraser University, Burnaby, BC, Canada
- ¹⁴⁵ SLAC National Accelerator Laboratory, Stanford, CA, United States
- ¹⁴⁶ ^(a) Faculty of Mathematics, Physics & Informatics, Comenius University, Bratislava; ^(b) Department of Subnuclear Physics, Institute of Experimental Physics of the Slovak Academy of Sciences, Kosice, Slovak Republic
- ¹⁴⁷ ^(a) Department of Physics, University of Cape Town, Cape Town; ^(b) Department of Physics, University of Johannesburg, Johannesburg; ^(c) School of Physics, University of the Witwatersrand, Johannesburg, South Africa
- ¹⁴⁸ ^(a) Department of Physics, Stockholm University; ^(b) The Oskar Klein Centre, Stockholm, Sweden
- ¹⁴⁹ Physics Department, Royal Institute of Technology, Stockholm, Sweden
- ¹⁵⁰ Departments of Physics & Astronomy and Chemistry, Stony Brook University, Stony Brook, NY, United States
- ¹⁵¹ Department of Physics and Astronomy, University of Sussex, Brighton, United Kingdom
- ¹⁵² School of Physics, University of Sydney, Sydney, Australia
- ¹⁵³ Institute of Physics, Academia Sinica, Taipei, Taiwan
- ¹⁵⁴ Department of Physics, Technion: Israel Institute of Technology, Haifa, Israel
- ¹⁵⁵ Raymond and Beverly Sackler School of Physics and Astronomy, Tel Aviv University, Tel Aviv, Israel
- ¹⁵⁶ Department of Physics, Aristotle University of Thessaloniki, Thessaloniki, Greece
- ¹⁵⁷ International Center for Elementary Particle Physics and Department of Physics, The University of Tokyo, Tokyo, Japan
- ¹⁵⁸ Graduate School of Science and Technology, Tokyo Metropolitan University, Tokyo, Japan
- ¹⁵⁹ Department of Physics, Tokyo Institute of Technology, Tokyo, Japan
- ¹⁶⁰ Department of Physics, University of Toronto, Toronto, ON, Canada
- ¹⁶¹ ^(a) TRIUMF, Vancouver, BC; ^(b) Department of Physics and Astronomy, York University, Toronto, ON, Canada
- ¹⁶² Faculty of Pure and Applied Sciences, University of Tsukuba, Tsukuba, Japan
- ¹⁶³ Department of Physics and Astronomy, Tufts University, Medford, MA, United States
- ¹⁶⁴ Centro de Investigaciones, Universidad Antonio Nariño, Bogotá, Colombia
- ¹⁶⁵ Department of Physics and Astronomy, University of California Irvine, Irvine, CA, United States
- ¹⁶⁶ ^(a) INFN Gruppo Collegato di Udine, Sezione di Trieste, Udine; ^(b) ICTP, Trieste; ^(c) Dipartimento di Chimica, Fisica e Ambiente, Università di Udine, Udine, Italy
- ¹⁶⁷ Department of Physics, University of Illinois, Urbana, IL, United States
- ¹⁶⁸ Department of Physics and Astronomy, University of Uppsala, Uppsala, Sweden
- ¹⁶⁹ Instituto de Física Corpuscular (IFIC) and Departamento de Física Atómica, Molecular y Nuclear and Departamento de Ingeniería Electrónica and Instituto de Microelectrónica de Barcelona (IMB-CNM), University of Valencia and CSIC, Valencia, Spain
- ¹⁷⁰ Department of Physics, University of British Columbia, Vancouver, BC, Canada
- ¹⁷¹ Department of Physics and Astronomy, University of Victoria, Victoria, BC, Canada

- ¹⁷¹ Department of Physics, University of Warwick, Coventry, United Kingdom
- ¹⁷² Waseda University, Tokyo, Japan
- ¹⁷³ Department of Particle Physics, The Weizmann Institute of Science, Rehovot, Israel
- ¹⁷⁴ Department of Physics, University of Wisconsin, Madison, WI, United States
- ¹⁷⁵ Fakultät für Physik und Astronomie, Julius-Maximilians-Universität, Würzburg, Germany
- ¹⁷⁶ Fachbereich C Physik, Bergische Universität Wuppertal, Wuppertal, Germany
- ¹⁷⁷ Department of Physics, Yale University, New Haven, CT, United States
- ¹⁷⁸ Yerevan Physics Institute, Yerevan, Armenia
- ¹⁷⁹ Centre de Calcul de l'Institut National de Physique Nucléaire et de Physique des Particules (IN2P3), Villeurbanne, France

- ^a Also at Department of Physics, King's College London, London, United Kingdom.
- ^b Also at Institute of Physics, Azerbaijan Academy of Sciences, Baku, Azerbaijan.
- ^c Also at Novosibirsk State University, Novosibirsk, Russia.
- ^d Also at Particle Physics Department, Rutherford Appleton Laboratory, Didcot, United Kingdom.
- ^e Also at TRIUMF, Vancouver, BC, Canada.
- ^f Also at Department of Physics, California State University, Fresno, CA, United States.
- ^g Also at Department of Physics, University of Fribourg, Fribourg, Switzerland.
- ^h Also at Departamento de Física e Astronomia, Faculdade de Ciências, Universidade do Porto, Portugal.
- ⁱ Also at Tomsk State University, Tomsk, Russia.
- ^j Also at CPPM, Aix-Marseille Université and CNRS/IN2P3, Marseille, France.
- ^k Also at Università di Napoli Parthenope, Napoli, Italy.
- ^l Also at Institute of Particle Physics (IPP), Canada.
- ^m Also at Department of Physics, St. Petersburg State Polytechnical University, St. Petersburg, Russia.
- ⁿ Also at Chinese University of Hong Kong, China.
- ^o Also at Louisiana Tech University, Ruston, LA, United States.
- ^p Also at Institutio Catalana de Recerca i Estudis Avancats, ICREA, Barcelona, Spain.
- ^q Also at Department of Physics, The University of Texas at Austin, Austin, TX, United States.
- ^r Also at Institute of Theoretical Physics, Ilia State University, Tbilisi, Georgia.
- ^s Also at CERN, Geneva, Switzerland.
- ^t Also at Georgian Technical University (GTU), Tbilisi, Georgia.
- ^u Also at Ochadai Academic Production, Ochanomizu University, Tokyo, Japan.
- ^v Also at Manhattan College, New York, NY, United States.
- ^w Also at Hellenic Open University, Patras, Greece.
- ^x Also at Institute of Physics, Academia Sinica, Taipei, Taiwan.
- ^y Also at LAL, Université Paris-Sud and CNRS/IN2P3, Orsay, France.
- ^z Also at Academia Sinica Grid Computing, Institute of Physics, Academia Sinica, Taipei, Taiwan.
- ^{aa} Also at School of Physics, Shandong University, Shandong, China.
- ^{ab} Also at Laboratoire de Physique Nucléaire et de Hautes Energies, UPMC and Université Paris-Diderot and CNRS/IN2P3, Paris, France.
- ^{ac} Also at School of Physical Sciences, National Institute of Science Education and Research, Bhubaneswar, India.
- ^{ad} Also at Dipartimento di Fisica, Sapienza Università di Roma, Roma, Italy.
- ^{ae} Also at Moscow Institute of Physics and Technology State University, Dolgoprudny, Russia.
- ^{af} Also at Section de Physique, Université de Genève, Geneva, Switzerland.
- ^{ag} Also at International School for Advanced Studies (SISSA), Trieste, Italy.
- ^{ah} Also at Department of Physics and Astronomy, University of South Carolina, Columbia, SC, United States.
- ^{ai} Also at School of Physics and Engineering, Sun Yat-sen University, Guangzhou, China.
- ^{aj} Also at Faculty of Physics, M.V. Lomonosov Moscow State University, Moscow, Russia.
- ^{ak} Also at National Research Nuclear University MEPhI, Moscow, Russia.
- ^{al} Also at Institute for Particle and Nuclear Physics, Wigner Research Centre for Physics, Budapest, Hungary.
- ^{am} Also at Department of Physics, Oxford University, Oxford, United Kingdom.
- ^{an} Also at Department of Physics, Nanjing University, Jiangsu, China.
- ^{ao} Also at Institut für Experimentalphysik, Universität Hamburg, Hamburg, Germany.
- ^{ap} Also at Department of Physics, The University of Michigan, Ann Arbor, MI, United States.
- ^{aq} Also at Discipline of Physics, University of KwaZulu-Natal, Durban, South Africa.
- ^{ar} Also at University of Malaya, Department of Physics, Kuala Lumpur, Malaysia.
- ^{*} Deceased.